Acta Neuropathologica

Neutrophil recruitment to the brain in mouse and human ischemic stroke

--Manuscript Draft--

Manuscript Number:	ANEU-D-14-00663R2
Full Title:	Neutrophil recruitment to the brain in mouse and human ischemic stroke
Article Type:	Original Paper
Keywords:	leptomeninges, perivascular, brain, ischemia, rodent, human
Corresponding Author:	Anna M. Planas, PhD IIBB-CSIC, IDIBAPS Barcelona, SPAIN
Corresponding Author Secondary Information:	
Corresponding Author's Institution:	IIBB-CSIC, IDIBAPS
Corresponding Author's Secondary Institution:	
First Author:	Isabel Perez-de-Puig, PhD
First Author Secondary Information:	
Order of Authors:	Isabel Perez-de-Puig, PhD
	Francesc Miro-Mur, PhD
	Maura Ferrer-Ferrer, Master in Science
	Ellen Gelpi, MD, PhD
	Jordi Pedragosa, Master in Science
	Carles Justicia, PhD
	Xabier Urra, MD, PhD
	Angel Chamorro, MD, PhD
	Anna M. Planas, PhD
Order of Authors Secondary Information:	
Abstract:	Neutrophils are rapidly recruited in response to local tissue infection or inflammation. Stroke triggers a strong inflammatory reaction but the relevance of neutrophils in the ischemic brain is not fully understood, particularly in the absence of reperfusion. We investigated brain neutrophil recruitment in two murine models of permanent ischemia induced by either cauterization of the distal portion of the middle cerebral artery (c-MCAo) or intraluminal MCA occlusion (il-MCAo), and three fatal cases of human ischemic stroke. Flow cytometry analyses revealed progressive neutrophil recruitment after c-MCAo, lesser neutrophil recruitment following il-MCAo, and absence of neutrophils after sham-operation. Confocal microscopy identified neutrophils in the leptomeninges from 6h after the occlusion, in the cortical basal lamina and cortical Virchow-Robin spaces from 15h, and also in the cortical brain parenchyma at 24h. Neutrophils showed signs of activation including histone-3 citrullination, chromatin decondensation, and extracellular projection of DNA and histones suggestive of extracellular trap formation. Perivascular neutrophils were identified within the entire cortical infarction following c-MCAo. After il-MCAo, neutrophils prevailed in the margins but not the center of the cortical infarct, and were intraluminal and less abundant in the striatum. The lack of collaterals to the striatum and a collapsed pial anastomotic network due to brain edema in large hemispheric infarctions could impair neutrophil trafficking in this model. Neutrophil extravasation at the leptomeninges was also detected in the human tissue. We concluded that neutrophils extravasate from the leptomeningeal vessels and can eventually reach the brain in experimental animal models and humans with prolonged arterial occlusion.

Answers to Reviewers R2

We are indebted to the Reviewers for their suggestions and time for the revision. We believe their comments have helped us to improve our manuscript very much. In this second revision we have been very careful to edit the nomenclature to avoid confusion and we have addressed all the concerns raised by the Reviewers. Reviewer 2 asked for more images illustrating the regional location of neutrophils in the il-MCAO model. To fulfill this request we have added a new Figure (new Figure 4). Reviewer 3 asked to remove one of the patients. Although we still believe the information of this patient was valuable, we agree it is a clinically complex case. To avoid this confusion we have followed the suggestion of the Reviewer and have removed this patient. Therefore a number of panels in previous Figures 5 and 6 had to be removed. For this reason we have constructed a new Figure showing microscopic H&E images of stroke patients combining the information of previous Fig. 5 and 6 and substituting images of the patient that was removed by images of the other patients.

In brief, in spite of adding a new Figure (new Fig. 4) to illustrate regional neutrophil location in the animal models, we ended up with the same number of Figures as in the revised version 1 after merging previous Figures 5 and 6 into one single Figure (new Fig. 6). Although we have included some text explaining the differences between the animal models, as requested by Reviewer 2, we have shortened the Discussion and the length of the manuscript has not been increased.

Reviewer #2

We are very glad the Reviewer believes that our revised version was improved. We thank again his/her critical work revising our manuscript. Here below are the answers to the specific concerns.

it is still rather difficult to understand the value of this comparative analysis as the precise localization of the blood vessels and leukocyte accumulations shown in the different MCAO models often remains unclear. In addition due to the imprecisions in nomenclature used by the authors it remains unclear if the conclusions drawn about localization of leukocytes hold. As the study aims to highlight potential differences in the two different permanent MCAO models I consider providing this information in great detail as absolutely essential.

In this revised version of our manuscript we have carefully addressed the requested differences between the two models. We have added a new Figure (new Figure 4) to illustrate the regional localization of neutrophils in the two models and we have added a section in Results on the Regional localization of neutrophils (page 12). Regarding the differences between the two models:

A distal portion of the MCA is occluded by cauterization in the c-MCAo model, which only affects the cortex. In this model, neutrophils were seen extravasated from leptomeningeal vessels, and on the basal lamina of the cortex, but neutrophils were only seen in the cortical perivascular spaces within the infarcted tissue. Likewise, neutrophils only extravasated to the parenchyma within the infarcted cortex, but were not identified in the neighboring non-affected tissue.

In the il-MCAo model the MCA is occluded at its origin in the circle of Willis and results in a large infarction involving the entire MCA territory (cortex and striatum). Neutrophils were comparatively less abundant in this model. They were also seen in the leptomeninges, on

the cortical brain surface, in perivascular spaces of cortical vessels, and, to a lower extent, extravasated in the brain parenchyma. However, they were more prevalent at the margins of the infarction (ventral and dorsal parts) (please see new Fig. 4) than in the infarcted core. In the infarcted striatum, neutrophils were seen inside the vessels rather than in perivascular spaces, and neutrophil extravasation was very infrequent in this region.

Several reasons might account for these differences between models, as we discussed in the revised manuscript. One main reason is that only a distal portion of the MCA is occluded in the c-MCAo model while the entire MCA is occluded in the il-MCAo model. After distal occlusion, proximal branches of the MCA remain patent and can supply neutrophils to the cortical surface. In contrast, in the il-MCAo model, all the MCA branches are occluded and therefore blood supply to the pial network is impaired. Another important difference between the c-MCAo model and the il-MCAo model is the edema that can expectedly develop in the il-MCAo model due to the much larger hemispheric infarction.

We added the following texts in the manuscript to address the model differences:

- Abstract: *'Perivascular neutrophils were identified within the entire cortical infarction following c-MCAo. After il-MCAo, neutrophils prevailed in the margins but not the center of the cortical infarct, and were intraluminal and less abundant in the striatum. The lack of collaterals to the striatum and a collapsed pial anastomotic network due to brain edema resulting from large hemispheric infarctions could impair neutrophil trafficking in this model*.'

-Results (page 12): '*In the c-MCAo model, the distal portion of the MCA is occluded resulting in a cortical infarction (Fig. 4a). Neutrophils were seen in the leptomeninges of the ipsilateral cortex and in the infarcted tissue, but were not detected in neighboring non-infarcted tissue (Fig. 4 b,c). In the il-MCAo model, the MCA is occluded at its origin in the circle of Willis and the resulting infarction affects the cortex and the striatum (Fig. 4d). In this model, neutrophils were seen within the infarcted cortex and were more prominent at the boundaries of the cortical infarction than in the core. They were seen in cortical perivascular spaces and extravasated to the parenchyma in ventral and dorsal parts of the cortex (Fig. 4e-h). In the striatum, which lacks collateral flow, most Ly6G+ cells were located in the vessel lumen and extravasation to the infarcted parenchyma was very rare (Fig. 4i). Occasionally, a few neutrophils were seen in the choroid plexus and the surrounding white matter (Fig. 4j).'*

- Discussion (bottom of page 18): '*Several differences in the ischemia models might account for the differences in neutrophil infiltration. il-MCAo induces occlusion of the entire MCA tree, while only the distal portion of the MCA is occluded in the c-MCAo model. Therefore, the leptomeningeal branches of the proximal portion of the MCA are patent after c-MCAo and can supply neutrophils to the anastomotic network of pial arteries near the cortical infarction. In contrast, in the il-MCAo model, the access of neutrophils to the leptomeninges of the ischemic territory would be limited to possible anastomoses of pial arterioles with branches from the external carotid artery and with collateral vessels from other arterial trees. Another important difference between these experimental models is the intracranial pressure that can develop after il-MCAo due to edema, which is comparatively negligible after c-MCAo as a consequence of partial craniectomy. It is possible that increased edema and intracranial pressure in this model would impair neutrophil trafficking to the core of the cortical ischemic region.* '

We have revised in detail the nomenclature trough the text to improve precision taking into account the specific comments of the Reviewer in the next questions.

The weaker part of this study remains the analysis of the human stroke tissue due to limited definition of the infiltrating cells (MPO does not allow to define neutrophils in CNS inflammation).

We cannot overcome the lack of infallible markers for neutrophil immunostaining in human samples. However, we believe that the histological hallmarks used by neuropathologists are also helpful. For this reason the human samples were studied by an expert neuropathologist (E.G.). The histological features of the cells, together with the presence of MPO and elastase provide support to the notion that neutrophils extravasate at the leptomeninges, access perivascular spaces and a few neutrophils reach the parenchyma of the infarcted tissue during the first days after stroke.

Reviewer 3 asked to remove one patient and we had to redo the Figures showing the human tissue substituting the images of that patient from images of the other patients. Please see new Figure 6 showing hematoxylin and eosin images that we believe that convincingly show the presence of polymorphonuclear cells.

Although the authors provide more information on the localization of the regions of analysis of the c-MCAO model in Supplementary Figure 4, this information has not been disclosed for the il-MCAO model.

As we described above, we generated a new Figure that is now presented in the main Figures (not Supplementary) where we provide information about the regional location of neutrophils in both models (please see new Fig. 4). In addition we added a section in Results on the comparative regional location of neutrophils in the two models (see page 12). Please also see our response to the first question.

Furthermore, although the authors did write in their point-by-point reply that they will improve reference to the brain regions analyzed - infarct core versus peripheral infarct zone - in the revised manuscript this information has not been consequently included in the text or the figure legends. Thus - it still remains rather difficult to appreciate the comparative analysis of the two MCAO models now shown in Figures 2 and 3 separately. To give some expamples: It is still impossible to understand if e.g. Figures 2a and g are localized in the core of the c-MCAO lesion or if in Figure 3 the leptomeningeal brain lesions analyzed are ventral or dorsal etc etc.

We regret we did not succeed explaining the regional localization of neutrophils in the brain. We hope the new Figure (Fig. 4) (see in the previous response) and the added text (see our response to the first question) will help to clarify this matter.

As mentioned in the response to the first question we modified several parts of the manuscript to clarify these findings.

Fig. 2a and g correspond to the core of infarction. This information has been added to the Figure legend.

In Figure 3 the leptomeningeal brain lesions analyzed are ventral in panels a-c, f, i and j, and dorsal in panels d, h, o, and p. Explanation about the regional localization has been added to Fig. 3 legend.

Confusion about the description of the localization of vessels and leukocytes analyzed is further increased by the imprecise nomenclature used by the authors. As this causes doubts about the interpretations of the results a clear nomenclature needs to be used. To name a few examples:

1. What do the authors mean by " the leukocytes cross the external basal lamina AND the glia limitans". (Figure legend 2). I was under the impression that with external basal lamina they refer to the parenchymal basal lamina, as this is however part of the glia limitans and the authors also refer in other places to the parenchymal basal lamina (Figure 3) this is simply confusing and does not allow the reader to understand the descriptions provided by the authors.

Thanks for pointing this issue. We certainly meant the parenchymal basal lamina and we have changed the terms in Figure legend 2, as suggested.

2. How did the authors define subpial vessels and distinguish them from subarachnoidal vessels?

We considered that the vessels were subpial when in coronal brain sections were immediately adjacent to the surface of the brain (e.g. Fig. 2n). Subarachnoid vessels tend to be larger and do not keep well attached to the surface of the brain in the cryostat sections and they are often seen partially separated of the brain tissue, or they are lost in the histological process. However, it is certain that we did not carry out a specific study to identify those vessels and therefore we changed the specific names of *subpial vessels* to *leptomeningeal vessels* in the figures.

3. Results page 10: "NIMP-R14+ cells were detected in the leptomeninges and the subarachnoid and subial spaces…". What do the authors mean when differentiating between leptomeninges and subarachnoid space?

With this sentence we wanted to distinguish the spaces in between the meningeal layers, but to avoid confusion we changed the sentence to:

"NIMP-R14+ cells were detected extravasated from leptomeningeal vessels of the ipsilateral hemisphere…".

4. Discussion. "From the subpial space the the cells can reach the external basal lamina of the cortex" - please define external basal lamina as compared to parenchymal basal lamina.

According to previous comments above, we have changed the term to *parenchymal basal lamina*.

Specific questions:
Figures 2 n and o: The authors refer in these figures to subpial and subarachnoid vessels employing staining for PDGFRbeta, which is a pericyte marker. Numerous neutrophils are found on what seems to be the surface of the brain (core or periphery of the lesion reamins unclear?) and the blue staining shows a continous outline of what rather looks like a laminin staining. 2o - does the PDGFRbeta staining in the top right corner mark the border of the tissue? Is the tissue ruptured or do we look at a true space between the pericyte layers?

Yes, this is correct. PDGFRb immunostaining marked the meningeal layers surrounding the meningeal vessels. Please notice that besides pericytes, expression of PDGFRb has also been reported in perivascular fibroblasts (Soderblom et al., 2013; Brachvogel et al., 2007).

The staining in Fig. 2n and o is PDGFRb. Regarding Figure 2o, the top right corner layer + for PDGFRb corresponds to a meningeal layer.

References:

Soderblom C, Luo X, Blumenthal E, Bray E, Lyapichev K, Ramos J, Krishnan V, Lai-Hsu C, Park KK, Tsoulfas P, Lee JK. Perivascular fibroblasts form the fibrotic scar after contusive spinal cord injury. J Neurosci. 2013 Aug 21;33(34):13882-7.

Brachvogel B, Pausch F, Farlie P, Gaipl U, Etich J, Zhou Z, Cameron T, von der Mark K, Bateman JF, Pöschl E. Isolated Anxa5+/Sca-1+ perivascular cells from mouse meningeal vasculature retain their perivascular phenotype in vitro and in vivo. Exp Cell Res. 2007 Jul 15;313(12):2730-43.

Figure 2p: The area around the vessel to the left is black however the area depicting a neutrophil to the right is sourrounded by faint a4-laminin and blue-pan laminin staining.

We checked the image at high magnification and we agree, the left side of the neutrophil shown in the right hand side of the image is adjacent to a faint a4-laminin stained vessel and this border of the neutrophil is rather flat suggesting that it might be adjacent to the vessel wall. Therefore, it is possible that it is located perivascularly. No doubt about the extensive perivascular location of neutrophils. This does not mean it is the case for all neutrophils. Please see in other images the presence of neutrophils in the parenchyma separated from the vessels. We would like to stress that neutrophil extravasation to the parenchyma was only seen in the cortex after long-lasting periods of ischemia and mainly in the c-MCAO model.

Figure 2r: Where is this vessel - in the core or the periphery of the lesion?

It is in the core. This is now stated in the figure legend.

Figure 2t: the vessel pointed out to accumulate neutrophils does not show a4-laminin staining. Considering the bright a4-laminin IF signal of the adjacent vessle this is confusing.

The intensity of a4-laminin is not even in all the vessels. The vessel showing neutrophil accumulation in the image (Fig. 2t) does show a4-laminin immunoreactivity but with lower intensity than vessels on the right hand side of this image. We have increased the intensity of the red color to show that a4-laminin was also present in this vessel and have modified the intensity of the image color to better illustrate it.

Figure 3c: Is this ventral or dorsal?

It is ventral and this is now stated in the Figure legend.

More confusion is added by the fact that in the Results describing the il-MCAO model there is still reference to Figure 2, which cannot be as this now solely showing c-MCAO. Please check if this is a simplex mix up e.g. referring to Figure 2d and meaning 3d.

We apologize for the confusion, we meant Fig. 3d and have changed the text accordingly.

Figures 5 and 6: Size bars should be given rather than magnifications, which will change during figure processing.

We now provide the scale bars, as suggested.

Reviewer #3: The authors carefully revised the manuscript which has substantially improved. In particular the additional data with a permanent ischemia by ligature of the MCA have elegantly solved the criticism of reviewer #3.

This reviewer has only one further suggestion. Although the authors toned down their findings in the human stroke patients as a proof of concept and although it is clear to the reviewer that it is very difficult to get ideal human samples I would strongly suggest removing the case with two subsequent infarcts and thrombolytic treatment of the first one due to too many variables with unknown effects.

We are glad the Reviewer appreciated the previous answers to his/her questions. Regarding the human case with two infarctions, we still believe it is valuable, but we agree that it is a complex case that could induce some confusion. In view of this comment we have removed this case. Consequently, we have removed all the pictures from this patient and excluded this case of the neutrophil counts in Fig. 7. We decided to merge previous figure 5 and 6 showing the H&E images in one figure (new Fig. 6) where we show images of the three patients that are now reported in this manuscript.

Isabel Perez-de-Puig[1&], Francesc Miró-Mur[2&], Maura Ferrer-Ferrer[1,2], Ellen Gelpi[3], Jordi Pedragosa[1], Carles Justicia[1,2], Xabier Urra[2,4], Angel Chamorro[2,4], Anna M. Planas[1,2]*

Neutrophil recruitment to the brain in mouse and human ischemic stroke

[1] Department d'Isquèmia Cerebral i Neurodegeneració, Institut d'Investigacions Biomèdiques de Barcelona (IIBB), Consejo Superior de Investigaciones Científicas (CSIC), Barcelona, Spain.

[2] Institut d'Investigacions Biomèdiques August Pi i Sunyer (IDIBAPS), Barcelona, Spain

[3] Neurological Tissue Bank of the Biobanc-Hospital Clinic- IDIBAPS, Barcelona, Spain.

[4] Functional Unit of Cerebrovascular Diseases, Hospital Clínic, Barcelona, Spain

& These authors equally contributed to this work

*** Corresponding author:**

Anna M. Planas, PhD
IIBB-CSIC, IDIBAPS
Rosselló 161, planta 6
08036-Barcelona, Spain
E-mail: anna.planas@iibb.csic.es
Phone: +34-93 363 83 27
Fax: +34-93 363 83 01

Abstract

Neutrophils are rapidly recruited in response to local tissue infection or inflammation. Stroke triggers a strong inflammatory reaction but the relevance of neutrophils in the ischemic brain is not fully understood, particularly in the absence of reperfusion. We investigated brain neutrophil recruitment in two murine models of permanent ischemia induced by either cauterization of the distal portion of the middle cerebral artery (c-MCAo) or intraluminal MCA occlusion (il-MCAo), and three fatal cases of human ischemic stroke. Flow cytometry analyses revealed progressive neutrophil recruitment after c-MCAo, lesser neutrophil recruitment following il-MCAo, and absence of neutrophils after sham-operation. Confocal microscopy identified neutrophils in the leptomeninges from 6h after the occlusion, in the cortical basal lamina and cortical Virchow-Robin spaces from 15h, and also in the cortical brain parenchyma at 24h. Neutrophils showed signs of activation including histone-3 citrullination, chromatin decondensation, and extracellular projection of DNA and histones suggestive of extracellular trap formation. Perivascular neutrophils were identified within the entire cortical infarction following c-MCAo. After il-MCAo, neutrophils prevailed in the margins but not the center of the cortical infarct, and were intraluminal and less abundant in the striatum. The lack of collaterals to the striatum and a collapsed pial anastomotic network due to brain edema in large hemispheric infarctions could impair neutrophil trafficking in this model. Neutrophil extravasation at the leptomeninges was also detected in the human tissue. We concluded that neutrophils extravasate from the leptomeningeal vessels and can eventually reach the brain in experimental animal models and humans with prolonged arterial occlusion.

Keywords: leptomeninges, perivascular, brain, ischemia, rodent, human.

Introduction

The only treatment showing efficacy in acute ischemic stroke is thrombolysis with recombinant tissue plasminogen activator (tPA) when it is administered within the first 4.5 hours after symptom onset. However, a majority of stroke patients arrive to the hospital later than 4.5 hours and cannot be treated with tPA [16]. It is estimated that spontaneous recanalization of the occluded vessel occurs in only one quarter of the stroke population by 24 hours of clinical onset [46] and in up to half of the patients by 1 week [39, 51]. However, the benefits derived from such a protracted recanalization are negligible. In sharp contrast with these data that illustrate that the archetypical stroke patient in the clinic suffers long lasting or permanent ischemia, most experimental studies are performed using experimental models of transient brain ischemia [29].

Acute ischemic stroke is a hypoxic-ischemic disorder associated with a sterile inflammatory reaction [7]. Ischemic injury triggers an immune response that promotes immune cell migration and infiltration to the brain parenchyma according to an orchestrated temporal pattern [23, 30]. Neutrophils have received special attention for many years as these cells have a remarkable destructive potential, either through the direct neurotoxic effects from the release of proteolytic enzymes [1, 48], or through indirect effects that result from intravascular neutrophil accumulation, capillary blood flow obstruction and the no-reflow phenomenon [14, 15]. Experimental studies showed that neutrophils migrate to cerebral ischemic regions during the first few hours after the onset of ischemia. However, they have not determined the exact anatomic location of neutrophil infiltration within the neurovascular unit and brain parenchyma [4, 15, 22, 24, 52]. More recently, it has been disputed whether neutrophils are able to cross the multiple physical barriers in the blood-brain barrier (BBB) that separate the intracerebral vessel lumen from the brain parenchyma after ischemia/reperfusion, or whether neutrophils penetrate the parenchyma in sufficient

numbers to be of clinical significance [18]. Alternatively, it has been posited that the neurovascular unit is the site of neutrophil action after CNS ischemia/reperfusion [18].

So far, interventions aiming to prevent neutrophil recruitment to the ischemic brain have not shown benefits in human stroke [34]. In experimental animals, several lines of evidence support a pathogenic role of neutrophils in ischemia/reperfusion but not in permanent ischemia [9, 10, 21, 32, 45, 53]. However, increased numbers of neutrophils have been detected after permanent brain ischemia and infiltration into the parenchyma was found to begin 12 hours after the onset of the arterial occlusion [8, 22, 52]. Remarkably, increasing data attest that neutrophils cross talk and shape the maturation and effector functions of other leukocytes, show diverse phenotypes [12, 19], and could play an important role in several pathological conditions [31, 36, 40]. In this study, we investigated the route of entry of neutrophils to the brain while the circulation remained arrested in experimental models of permanent occlusion of the middle cerebral artery (MCAo) in mice. In addition, we assessed the anatomical localization of neutrophil infiltration in fatal cases of human stroke.

Methods

Animals

Adult (3-4 month-old) Balb/C male mice (n=89) were purchased from Charles River (Lyon, France). Animal work was carried out according to the local regulations and in compliance with the Spanish laws (Real Decreto 53/2013) following the Directives of the European Community and with approval of the Ethics Committee (CEEA) of University of Barcelona.

Brain ischemia

Focal brain ischemia was induced by permanent right MCAo in mice, either by cauterization of the distal portion of the MCA (c-MCAo) (n=43), or by intraluminal MCA occlusion (il-

MCAo) (n=28). c-MCAo restricts blood flow within a limited portion of the cortex, whereas il-MCAo affects the entire MCA territory causing striatal and cortical infarctions. A detailed description of the experimental procedures is provided in the *Supplementary Materials*. In brief, c-MCAo was carried out under isoflurane anesthesia as reported [43]. Two mice were excluded from the study due to unsuccessful surgery. None of the mice died during the study. For sham-operation (n=7), all surgical procedures were carried out but the MCA was not cauterized and the mice were killed at 24 hours. To exclude any effects of cauterization, in a small group of mice (n=3) we carried out MCA ligature (8/0 black-braided silk suture) and the mice were studied at 24 hours. il-MCAo was performed under isoflurane anesthesia introducing a filament through the right internal carotid artery up to the level where the MCA branches out, as reported [13] with modifications. Cerebral perfusion was assessed with laser Doppler flowmetry (Perimed AB, Järfälla Sweden). Three mice died before 24 hours after il-MCAo. Sham-operated mice (n=4) were subjected to surgery but the filament was only briefly introduced into the internal carotid artery and was immediately removed, and mice were killed after 24 hours. Control mice (n=4) were naïve mice not subjected to surgery or anesthesia.

Isolation of cells from tissues

Mice were anesthetized and transcardially perfused with 40 mL saline. The ischemic brain tissue (ipsilateral to the MCAo) and the identical regions of the non-ischemic hemisphere (contralateral) were dissected out and analyzed separately. For the c-MCAo model the cortex was dissected out, whereas for the il-MCAo model the dissected tissue included the cortex and the striatum. The tissue was processed to obtain cells as described in *Supplementary Materials*.

Flow cytometry

Isolated brain cells were processed as described in the *Supplementary Materials* and incubated with the following primary antibodies: rat anti-mouse CD11b (clone M1/70, Alexa Fluor 647, BD Pharmingen), CD45 (clone 30-F11, FITC, BD Pharmingen), and Ly6G (clone 1A8, PE-Cy7, BD Pharmingen). Isotype controls were rat IgG2bκ (clone A95-1, Alexa Fluor 647 or FITC, BD Pharmingen), rat IgG2a (FITC, Hycult Biotech), and rat IgG2aκ (clone R35-95, PE-Cy7, BD Pharmingen). Data acquisition was carried out in a BD FacsCantoII cytometer (BD Biosciences) using the FacsDiva software (BD Biosciences). Data analysis was carried out with FlowJo software (version 7.6.5, TreeStar Inc., Ashland, OR, USA). Flow-Count Fluorospheres (Beckman-Coulter) were used for absolute cell number quantification.

Immunofluorescence

Mice were anesthetized with isoflurane and perfused intracardially with saline followed by paraformaldehyde (PFA, 4%) in phosphate buffer (pH 7.4). The brain was removed, post-fixed with PFA overnight, cryoprotected in 30% sucrose, frozen, and 14 µm-thick sections were obtained in a cryostat. The sections were fixed with ethanol, blocked with normal serum and incubated overnight at 4ºC with combinations of primary antibodies (See Table 1). We generally combined antibodies made in different species to avoid cross-reactions. Then, sections were incubated for 2 hours at room temperature with secondary antibodies (Alexa Fluor-488, -546, -647, LifeTechnologies). Immunoreaction controls were always carried out by omission of the primary antibodies. Sections were counterstained with either 4',6-diamidino-2-phenylindole (DAPI) or ToPro-3 (Invitrogen) to visualize the cell nuclei and they were observed under a confocal laser microscope (Leica, SP5 or TCS SPE).

Post-mortem tissue of stroke patients

The brains of three patients suffering from acute stroke who died between 1-5 days after stroke onset at the Stroke Unit of the Hospital Clinic of Barcelona were used in this study, after obtaining written consent from their families for tissue removal after death for diagnostic and research purposes at the Neurological Tissue Bank of the Biobank-Hospital Clinic-*Institut d'Investigacions Biomèdiques August Pi i Sunyer* (IDIBAPS). The study had the approval of the Ethics Committee of this Hospital. The patients included two women and one man, and had a mean age of 84.7 years (ranging from 79 to 89 years). A summary of the characteristics of the patients is shown in Table 2. All patients had radiologically confirmed ischemic infarcts. These infarcts affected the territory of the middle cerebral artery in one case and the cerebellum in two cases (*Supplementary Fig. 1*). The elapsed time from stroke onset to death ranged from 1 to 5 days, and the time from death to autopsy ranged from 3 to 4 hours. An expert neuropathologist (EG) dissected the ischemic core, the peripheral region, the leptomeninges, and a portion of non-ischemic tissue obtained from an unaffected region distant to the infarction (*Supplementary Fig. 2*). Samples of the tissue from each region were either formalin-fixed, paraffin-embedded and sectioned in a microtome at 5 μm, or embedded in OCT and immediately frozen in liquid nitrogen for later sectioning in a cryostat at 5 μm. Paraffin sections were stained with hematoxylin and eosin, or were used for immunohistochemistry applying a rabbit polyclonal antibody against myeloperoxidase (Table 1), and processed with the avidin-biotin-peroxidase (ABC, Vector, Vectastain, Palex Medical S.A., Sant Cugat del Vallés, Spain) method. Cryostat sections were processed for immunofluorescence as described above with the antibodies listed in Table 1. For cell counting, we obtained 5-6 immunofluorescence pictures for each brain region using the x40 objective in two different sections. The numbers of immunoreactive cells located either within the vessel lumen (intravascular), surrounding the vascular endothelium (perivascular), or in the parenchyma (extravascular) were counted in each picture. The average counts in all pictures was taken as representative for each region per subject.

Statistical analyses

Cell numbers at different time points were compared with two-way ANOVA. For the il-MCAo model, comparisons between two groups were carried out with the Mann-Whitney U test. Cell numbers in human samples were compared with the Kruskal-Wallis test followed by the Dunn's Multiple Comparison test. Data were analyzed using GraphPad software.

Results

Neutrophils reach the ischemic territory after permanent ischemia in mice

The presence of neutrophils in the ischemic brain has been reported in experimental models of permanent ischemia [8, 22, 52]. After intracardiac perfusion of the mice, isolation of cells from the brain, and flow cytometry analysis, we found neutrophils in the ipsilateral hemisphere 24 hours after permanent ischemia (Fig. 1). Given that blood within the branches of the occluded vessels is not washed out after intracardiac perfusion of the animals, we first asked whether the stagnated blood was the source of neutrophils in the infarcted tissue. To answer this question we carried out flow cytometry in brain tissue samples at different time points after induction of permanent ischemia by c-MCAo (Fig. 1a). The number of neutrophils (CD45+CD11b+Ly6G+ cells) in the ipsilateral hemisphere increased with time reaching a peak at 24 hours (Fig. 1c). This finding was not observed in the contralateral hemisphere or after sham-operation (Fig. 1c). For the intraluminal ischemia model (il-MCAo), FACS analysis of the ischemic tissue at 24 hours also showed increased numbers of neutrophils compared with the contralateral hemisphere and compared with tissue of sham-operated mice (Fig. 1d). Comparatively, neutrophils were less abundant after il-MCAo than after c-MCAo. c-MCAo requires invasive surgery involving partial craniectomy

and causing a hole in the leptomeninges to access the MCA for direct occlusion. Although surgery might contribute to the local presence of neutrophils in the leptomeninges, sham-operation, where all the surgical procedures excepting cauterization of the MCA were carried out, induced a negligible presence of neutrophils at 24 hours (Fig. 1c). In order to ensure that MCA cauterization was not the cause of neutrophil recruitment, we carried out direct occlusion of the MCA by means of a ligature. This procedure induced a large cortical infarction that was visually apparent when the brain was removed from the skull at 24 hours, and abundant neutrophils were detected in the ipsilateral hemisphere by FACS (mean±SEM number of cells per ischemic cortex = 21234±7524, n=3). Overall, this experiment showed that ischemia triggered neutrophil recruitment after direct occlusion of the MCA in the absence of reperfusion.

Neutrophils leave the circulation at the leptomeninges and invade perivascular spaces after c-MCAo

By confocal laser microscopy we found polymorphonuclear cells extravasated from leptomeningeal vessels, in the subpial space and on the parenchymal basal lamina of the ischemic cortex, and entering the Virchow-Robin spaces surrounding cortical vessels of the ischemic region six hours after c-MCAo (Fig. 2a). We then studied these cells by immunofluorescence using NIMP-R14 (Fig. 2b-l) and Ly6G (Fig. 2m-t) antibodies. The NIMP-R14 antibody is widely used to study neutrophils, but in fact it recognizes Ly6G and also Ly6C, which is expressed not only by neutrophils but also by a subpopulation of monocytes, and therefore can label infiltrating macrophages in addition to neutrophils. In contrast, the Ly6G+ cells are taken as neutrophils. Nonetheless, in the flow cytometry study we observed a subpopulation of Ly6G+ cells in the ischemic brain that were CD45+ but CD11b- (Fig. 1a), and therefore did not conform to the typical neutrophil phenotype. Although in

immunofluorescence the Ly6G antibody could recognize both Ly6G+CD11b+ (neutrophils) and Ly6G+CD11b- cells, only 4.5% of the total Ly6G+ cells were CD11b- at 24h post-ischemia according to the FACS analysis. This result showed that the majority of the Ly6G+ cells detected by immunofluorescence at 24h should be neutrophils.

NIMP-R14+ cells were detected extravasated from leptomeningeal vessels of the ipsilateral hemisphere from 6 hours following c-MCAo. NIMP-R14+ cells were seen around the cortical glia limitans in the proximity of the ischemic territory, and surrounding superficial cortical blood vessels located in the ischemic region (Fig. 2b-d), but not in the contralateral hemisphere (Fig. 2e, f). In the ischemic cortical territory, NIMP-R14+ cells were located in the perivascular spaces between the parenchymal basal lamina and the endothelium (Fig. 2g,k), and in many instances the shape of the cell nucleus was compatible with that of polymorphonuclear cells (e.g. Fig. 2g-z1). At 24 hours, NIMP-R14+ cells were abundant in the leptomeninges and on the parenchymal cortical basal lamina of the ipsilateral hemisphere (Fig. 2h,i) and invading the cavities of cortical arterioles located in the infarcted core (Fig. 2j). They were also seen extravasated to the infarcted parenchyma (Fig. 2l, m), while erythrocytes remained in the vessel lumen in the absence of overt hemorrhagic transformation (Fig. 2l).

With the antibody against Ly6G (Fig. 2n-u) we identified positive cells outside leptomeningeal vessels and adjacent to the parenchymal basal lamina of the ischemic cortex (Fig 2n, o). Ly6G+ cells were also seen in perivascular spaces of cortical vessels located between the parenchymal basal lamina (pan-laminin) and the endothelial basal lamina expressing α4-laminin (Fig. 2p, s). The parenchyma basal lamina seemed to contain the Ly6G+ cells during the early hours after MCAo, as previously reported [18]. After 24 hours, Ly6G+ cells were seen perivascularly and also extravasated to the parenchyma of the infarcted core, near the vessels (Fig 2 q, t, u) and mainly in superficial cortical layers (Fig. 2u).

Adhesion of intravascular NIMP-R14+ or Ly6G+ cells to post-capillary venules was occasionally observed, and these cells egressed to perivascular spaces and across the basal lamina (*Supplementay Fig 3a-d*). In addition, we detected NIMP-R14+ and Ly6G+ cells in the lumen of occluded capillaries (*Supplementary Fig. 3e-f*), presumably corresponding to neutrophils stagnated in the vessels of the ischemic region.

Neutrophils after permanent intraluminal occlusion of the MCA (il-MCAo)

For comparative purposes we also studied the permanent il-MCAo model by confocal laser microscopy. Immunofluorescence showed NIMP-R14+ cells surrounding veins and arteries of the leptomeninges and on the cortical parenchymal basal lamina (Fig. 3a-c) from 6 hours onwards, and in the perivascular spaces of large cortical vessels mainly at the margins of the ischemic core from 15 hours (Fig. 3d). At 24 hours, the NIMP-R14+ cells were observed not only perivascularly but also free in the cortical parenchyma in infarcted zones at the boundary of the infarcted core (Fig. 3e,f). However in the infarcted striatum, NIMP-R14+ cells were less abundant and were mainly located in the lumen of capillaries (Fig. 3g). Although in some instances it was apparent that the nuclear morphology of the NIMP-R14+ cells was in compliance with that of neutrophils (e.g. arrowheads in Fig. 3d,e), we carried out a study using the neutrophil-specific Ly6G antibody. Ly6G+ cells were seen on the cortical parenchymal basal lamina (Fig. 3h, o), the perivascular spaces of cortical vessels (Fig. 3i), and extravasated from leptomeningeal vessels (Fig. 3j, k). Some Ly6G+ cells were trapped in brain capillaries (Fig. 3l), while others were found in the cortical perivascular spaces between the endothelial basal lamina (α4-laminin+) and the parenchymal basal lamina (Fig. 3m, n). Some Ly6G+ cells were seen in the cortical infarcted parenchyma (Fig. 3n, q).

Comparative regional location of neutrophils between the c-MCAo and the il-MCAo models

In the c-MCAo model, the distal portion of the MCA is occluded resulting in a cortical infarction (Fig. 4a). Neutrophils were seen in the leptomeninges of the ipsilateral cortex and in the infarcted tissue, but were not detected in neighboring non-infarcted tissue (Fig. 4 b,c). In the il-MCAo model, the MCA is occluded at its origin in the circle of Willis and the resulting infarction affects the cortex and the striatum (Fig. 4d). In this model, neutrophils were seen within the infarcted cortex and were more prominent at the boundaries of the cortical infarction than in the core. They were seen in cortical perivascular spaces and extravasated to the parenchyma in ventral and dorsal parts of the cortex (Fig. 4e-h). In the striatum, which lacks collateral flow, most Ly6G+ cells were located in the vessel lumen and extravasation to the infarcted parenchyma was very rare (Fig. 4i). Occasionally, a few neutrophils were seen in the choroid plexus and the surrounding white matter (Fig. 4j).

Neutrophils showed signs of activation in the ischemic brain

Neutrophils have granules containing proteases, such as neutrophil elastase (*Supplementary Fig. 4*). Upon activation, these enzymes are released to the extracellular environment after neutrophil degranulation. As part of their antimicrobial function, neutrophils are known to project extracellular traps (NETs) releasing enzymes, histones, and DNA out of the cells, and die through a distinctive process called NETosis [2]. Prior to releasing NETs, neutrophil enzymes access the cell nucleus and promote chromatin decondensation [42] involving histone modifications. Histone citrullination is believed to be a hallmark of NET formation [49]. To identify signs of NET formation in the ischemic brain, we used an antibody against citrullinated histone 3 (Cit-H3). No Cit-H3 positive reactions were seen in the control brain or in the contralateral hemisphere (not shown). However, in both experimental MCAo models some neutrophils showed Cit-H3 positive labeling (Fig. 4). Cit-H3 neutrophils became

apparent after 24 hours of ischemia but were rare at earlier time points. Cit-H3+ neutrophils were located in perivascular spaces (Fig. 4a), in the brain parenchyma nearby blood vessels (Fig. 5b), and in the lumen of capillaries (Fig. 4c). In the c-MCAo model, we estimated that about 15-20% of the neutrophils were Cit-H3+ at 24 hours, and were found in all of the different locations described above. However, in the il-MCAo model, most of the Cit-H3+ neutrophils were located intravascularly, particularly in the striatum.

By examining the DNA in the Cit-H3 positive neutrophils (Ly6G+) we found some evidence of NET formation in the ischemic cortex at 24 hours (Fig. 4d-h). Certain Ly6G+ neutrophils showed the presence of DNA (DAPI) and Cit-H3 surrounding the cell body, suggesting projection of DNA and histones to the extracellular milieu (Fig. 4d). Other Cit-H3+ neutrophils lost their typical lobular nuclei and showed diffuse DNA staining indicative of chromatin decondensation (Fig. 4e). Extracellular DNA and histones were also observed adjacent to neutrophils located inside the capillary lumen (Fig. 4f). Occasionally NET-like structures were seen surrounding pericytes (PDGFRβ+) (*Supplementary Fig. 5*), suggesting that NETs might damage components of the BBB. Altogether, the confocal images strongly supported that after prolonged ischemia some neutrophils can expel DNA and other intracellular components out of the cells indicative of NET formation.

We searched for some evidence of caspase-dependent apoptosis by immunostaining for active caspase-3. Caspase-3+ cells were detected in the ischemic tissue but they did not co-localize with neutrophil markers (not shown). Although we cannot exclude that neutrophils undergoing cell death might down-regulate the typical membrane markers preventing their identification, our results provide evidence of NETosis and do not support that caspase-dependent apoptosis is involved in neutrophil death during the first 24 hours of ischemia.

Neutrophils in the post-mortem brain of stroke patients

We investigated the brain of 3 stroke patients that died within 1-5 days after stroke onset (see Table 2 for clinical case description and *Supplementary Fig. 1* for illustration of intracranial occlusion sites). In all of the patients, conventional histological staining (hematoxylin & eosin) of paraffin-embedded brain sections showed the presence of polymorphonuclear cells with typical features of neutrophils in the leptomeninges surrounding the ischemic tissue (Fig. 6a, e, g), but not in the leptomeninges located in distant non-affected areas (Fig. 6b). In the ischemic tissue, polymorphonuclear cells were found in perivascular spaces of brain vessels (Fig. 6c, d, f, h), and, to a lesser extent, free in the infarcted parenchyma (Fig. 6d, f, h), particularly at the boundaries of the infarcted tissue. Immunostaining of paraffin sections with myeloperoxidase (MPO) showed positive cells in the leptomeninges and the ischemic tissue, where they were seen inside the vessels, in perivascular spaces, and to a lesser extent, in the parenchyma (*Supplementary Fig. 6*).

Cryostat sections were stained for neutrophil elastase (NE) together with laminin. We observed NE+ cells in three different locations, i.e. intravascular (Fig. 7a), perivascular (Fig. 7b), and extravascular (Fig. 7c,d). MPO and NE co-localized in the same cells (Fig. 7e). We counted the numbers of NE+ cells in each of the above locations (Fig. 7f-h) within different brain regions: the core of infarction, the periphery, and a control non-affected region distant from the infarction, and in the leptomeninges surrounding ischemic and non-affected zones. The numbers of intravascular NE+ cells (Fig. 7f) were higher in the infarcted tissue and surrounding the leptomeninges than in the corresponding non-affected regions, but differences were only statistically significant for the leptomeninges (Fig. 7f). NE+ cells were also seen in perivascular spaces (Fig. 7g) and, to a lesser extent, free in the parenchyma within the infarct (Fig. 7h), but differences did not reach statistical significance when compared to the non-affected (control) regions presumably due to the small number of

patients and intra-group variability. Extravasated NE+ cells were detected in the leptomeninges surrounding the ischemic tissue, with statistically significant differences compared to distant leptomeninges (Fig. 7h).

Discussion

Neutrophils play an essential function in building up a rapid innate immune response against invading pathogens, but can also damage the tissues due to their high proteolytic enzyme content and capacity of generating reactive oxygen intermediates [27] and activating the complement system [41]. Therefore, neutrophil activation must be tightly regulated to avoid uncontrolled release of its intracellular content. Leukocyte access to the brain is prevented by the BBB, but under pathological conditions leukocytes can adhere to activated post-capillary venules and infiltrate the brain parenchyma across the BBB [17]. However, in ischemic stroke, blood flow is arrested and peripheral leukocytes cannot reach the ischemic territory through the circulation, unless they accessed it through collateral blood vessels, peripheral regions, or after the occluded vessels are reperfused. This is why it is generally believed that neutrophils play a more prominent role in ischemia/reperfusion than in permanent ischemia. In this study we found that the numbers of neutrophils present in the ischemic territory increased with time after permanent MCAo in rodents, in agreement with previous studies [8, 22]. Although we found evidence of neutrophil adhesion to the walls of post-capillary venules, we report that a major pathway through which neutrophils can invade the ischemic tissue during the arterial occlusion is via leaving the circulation at the leptomeningeal vessels. Neutrophils were seen in perivascular spaces of cortical arterioles. Inflammatory cells in the subarachnoid space are able to cross the pia matter and access the subpial space under certain pathological conditions [28]. From the subpial space the cells can reach the parenchymal basal lamina of the cortex and the perivascular spaces of cortical

arterioles, since the Virchow-Robin space is communicated to the subpial space [28, 37]. A previous intravital microscopy study showed the presence of rolling and adherent leukocytes in pial venules and in arterioles of the ischemic tissue after permanent focal cerebral ischemia in mice [33]. Our study identified neutrophils in these locations but has the limitation that the results were obtained from static microscopic images. *In vivo* imaging studies will be required to provide a full demonstration of the impact of this trafficking pathway in neutrophil recruitment after stroke. The presence of polymorphonuclear cells in the subarachnoid space, as assessed by classic histology, was reported after permanent intraluminal MCAo in rats [22], and a previous study in mice found Ly6G+ neutrophils in the leptomeninges and perivascular spaces after ischemia/reperfusion in mice [18]. Our results confirm the latter findings showing that the perivascular spaces are a niche for neutrophils after brain ischemia, and extend the findings to the situation of permanent ischemia showing that neutrophil extravasation at the leptomeninges provides a pathway for neutrophil recruitment to the ischemic cortical territory in the absence of reperfusion.

Typically, bacterial meningitis causes massive neutrophil infiltrates in the leptomeninges and intraparenchymal vasculitis is characterized by perivascular neutrophil infiltration [28, 35]. Although the effect is comparatively much more modest after stroke, some underlying molecular mechanism could be similar. Indeed, neutrophils sense the presence of pathogens but they also respond to danger signals and chemoattractants under sterile inflammation [7]. After stroke, chemokines and danger signals are released to the extracellular space [6, 30]. Interstitial fluid can drain through the perivascular spaces of cortical arterioles towards the leptomeninges and out of the brain [5, 11, 25, 50]. However, perivascular drainage appears to be mediated by arterial vessel pulsations [26] and it was found to be impaired during experimental ischemia [3]. This finding suggests that during ischemia the perivascular spaces of cortical arterioles might accumulate signals capable of attracting neutrophils. We found neutrophils in perivascular spaces of cortical ischemic regions but not in the infarcted

striatum. The anatomy of the periarterial spaces in the basal ganglia differs from that in the cerebral cortex [44], and the terminal vessels supplying blood to the subcortical regions lack collateral blood flow with adjacent arteries. In contrast, pial arterioles on the cortical surface form a rich anastomotic network. Regional differences in the anatomic structure of the specific vascular beds may condition the process of interstitial fluid drainage and the regional capacity to allow trafficking of inflammatory cells during the arterial occlusion.

Neutrophils progressively accumulated in the perivascular spaces as the duration of ischemia increased and the parenchymal basal lamina seemed to act as a containment barrier preventing the free passage of the neutrophils to the parenchyma, as was previously reported after ischemia/reperfusion [18]. However, after long periods of ischemia, we detected neutrophils extravasated to the cortical parenchyma, as previously described by classical histology after 12 hours of permanent intraluminal MCAo in rats [22]. Although isolated erythrocytes were occasionally detected in the parenchyma within the infarcted core at 24 hours likely due to capillary damage, the presence of neutrophils in the cortical parenchyma was observed in the absence of hemorrhagic transformation. Activated neutrophils cause vascular damage by generating oxidative stress [27] and complement activation [47], and neutrophil elastase enhances vascular permeability and is involved in ischemic brain damage [48]. It is feasible that perivascular neutrophils accessed the parenchyma after some of them suffered NETosis, involving the loss of their typical nuclear morphology, release of their content and cell death [2, 42]. Although the triggers of such changes are currently unknown, sustained hypoxia, or extravasation of plasma components or erythrocytes might play a role. Neutrophils were also found in the capillary lumen within the ischemic area in the cortex and striatum, likely remaining in the blood stagnated in the vessels after the arterial occlusion. After prolonged periods of ischemia, these intraluminal neutrophils also showed signs of NETosis. NETs formed in the blood promote coagulation and thrombosis [20, 38]. Therefore, intravascular NETosis might induce secondary

microthrombosis. These events might be relevant for delayed restoration of reperfusion when the duration of ischemia is long enough to allow intravascular NETosis to take place, and could contribute to the no-reflow phenomenon.

In this study, neutrophils were more abundant after c-MCAo than after il-MCAo. Although this observation could suggest that the surgery was involved in attracting neutrophils, such an effect was not seen after sham-operation, pointing to brain ischemia as the driver of neutrophil recruitment. Experimental stroke models normally involve surgery causing mechanical injuries to the tissues or arteries that could contribute to neutrophil recruitment. Alternatively, neutrophils can strongly respond to post-surgical local infection. However, neutrophils were found in the ischemic brain after taking high precaution in sterilizing surgical material and working under clean conditions, and they were focally localized in the ischemic zone. Furthermore, the mild functional deficits [43] and good general status of the mice after c-MCAo argue against the possibility of meningeal infection. Several differences in the ischemia models might account for the differences in neutrophil infiltration. il-MCAo induces occlusion of the entire MCA tree, while only the distal portion of the MCA is occluded in the c-MCAo model. Therefore, the leptomeningeal branches of the proximal portion of the MCA are patent after c-MCAo and can supply neutrophils to the anastomotic network of pial arteries near the cortical infarction. In contrast, in the il-MCAo model, the access of neutrophils to the leptomeninges of the ischemic territory would be limited to possible anastomoses of pial arterioles with branches from the external carotid artery and with collateral vessels from other arterial trees. Another important difference between these experimental models is the intracranial pressure that can develop after il-MCAo due to edema, which is comparatively negligible after c-MCAo as a consequence of partial craniectomy. It is possible that increased edema and intracranial pressure in this model would impair neutrophil trafficking to the core of the cortical ischemic region.

In human stroke, we identified the presence of polymorphonuclear cells in the leptomeninges proximal to infarction and in perivascular spaces of the ischemic tissue, but not in the non-affected territories. Cells with the characteristic morphology of neutrophils carrying the typical enzymes MPO and neutrophil elastase were seen in perivascular spaces of the infarcted tissue and to a lower extent extravasated from the vessels, but their numbers were comparatively more discrete than in the surrounding leptomeninges. In the human cases we have some evidence of permanent arterial occlusions but we are not certain about the precise status of blood flow at the time of death since imaging studies for research purposes cannot often be performed in critical stroke patients. This fact may be an important confounding factor given that, from the animal results, we would only expect substantial neutrophil infiltration to the parenchyma through the leptomeninges pathway after prolonged periods of ischemia. Nevertheless, the majority of patients that do not recanalize in the acute phase of stroke have long-lasting occlusions [39, 46, 51]. Although the small number of stroke patients and the heterogeneity of the infarcted territories are limitations of this study, we detected neutrophils in the leptomeninges proximal to the infarction in all the patients. This finding is a proof of concept that our experimental results could be relevant to human stroke.

In summary, we showed that during MCAo, neutrophils reached cortical brain territories devoid of blood flow after extravasating from leptomeningeal vessels surrounding the infarcted tissue and reaching the cortical parenchymal basal lamina as well as the perivascular spaces of cortical arterioles. After prolonged periods of ischemia, neutrophils became activated showing signs of NET formation inside the vessel lumen and around the blood vessels suggesting that the neurovascular unit is a target of action of neutrophils in stroke. The presence of neutrophils in the leptomeninges surrounding the infarcted regions was confirmed in postmortem human brain tissue supporting that this pathway is also relevant for neutrophil recruitment in human ischemic stroke.

ACKNOWLEDGEMENT

Supported by the Spanish Ministries of Economy (SAF2011-30492) and Health (FIS PI12/01437), and FP7 EU projects ERANET-NEURON (PRI-PIMNEU-2011-1342) and InMIND (grant agreement n°278850). We acknowledge Alba Hernández, Unai Perpiñá and Ana Guerrero for technical assistance. We thank the Cytometry and Image Platforms of IDIBAPS, and Dr. Maria Calvo and Anna Bosch of the Confocal Microscopy Unit of the *Serveis Cientifico-Tècnics* of the University of Barcelona for technical advice and support. We are indebted to the Neurological Tissue Bank of the Biobank-Hospital Clinic-IDIBAPS for sample and data procurement, and to patient's relatives for giving consent to this study. We thank Dr. Vanessa Brait for helpful comments and editing.

DISCLOSURES

The authors declare no disclosures.

Table 1. Antibodies for immunofluorescence

Antibody	species	reference	supplier	dilution
Anti-mouse				
Ly6G (clone 1A8) Recognizes neutrophils	rat monoclonal	127601	BIOLEGEND	1:200
Ly6G/C (NIMP-R14) Recognizes neutrophils and a subset of monocytes/macrophages	rat monoclonal	ab2557	ABCAM	1:100
Elastase Recognizes neutrophils and precursors, and certain monocytes express low levels	rabbit polyclonal	ab68672	ABCAM	1:50
Histone-3 citrulline Citrullination is a histone modification typical of neutrophil extracellular traps	rabbit polyclonal	ab5103	ABCAM	1:400
pan-Laminin Recognizes the laminin protein family widely expressed in basal laminae	Rabbit polyclonal	Z0097	DAKO	1:100
α4-Laminin Recognizes a laminin protein specific of the endothelial basal lamina	goat polyclonal	AF3837	R&D	1:20
PDGFRβ This PDGF receptor is mainly expressed in pericytes	goat polyclonal	AF1042	R&D	1:100
vWF Labels the vascular endothelium	sheep polyclonal	ab11713	ABCAM	1:100
Glut-1 Mainly labels the vascular endothelium	rabbit polyclonal	07-1401	MILLIPORE	1:200
CD31 Mainly labels the endothelial cells	mouse monoclonal	sc-46694	SANTA CRUZ	1:50
β-catenin Is involved in cell-cell adhesion, labels endothelial cell junctions	mouse monoclonal	61015	BD	1:500
Caspase-3 Apoptosis effector protein	rabbit polyclonal	ab52293	ABCAM	1:100
Anti-human				
Neutrophil elastase Recognizes neutrophils and precursors, and certain monocytes express low levels	mouse monoclonal	M0752	SEROTEC	1:200
Myeloperoxidase Enzyme found mainly in neutrophil primary granules and monocyte lysosomes	rabbit polyclonal	A 0398	DAKO	1:100
pan-Laminin Recognizes the laminin protein family widely expressed in basal laminae	rabbit polyclonal	Z0097	DAKO	1:200
vWF Labels the vascular endothelium	sheep polyclonal	ab11713	ABCAM	1:100

Table 2. Clinical data of the stroke patients

Case	Age	Gender	Admission NIHSS	Vascular territory	Intracranial occlusion site	Acute revascularization therapy	Hemorr-hagic transfor-mation (HT)	Etiology	Exitus (days after onset)	Exitus to necropsy timela	Acute infection
1	79	Man	4	Left MCA infarct	Left M2	None	Parieto-occipital parenchymal hematoma type 2	Large vessel disease	5 days	4 hours	No
2	86	Woman	1	Vertebro-basilar infarc	Basilar artery	None	No	Cardio-embolic	3 days	3 hours	Yes pneumonia
3	89	Woman	9	Vertebro-basilar infarct	No vessel imaging	None	No	Cardio-embolic	1 day	3 hours	Yes

REFERENCES

1. Allen C, Thornton P, Denes A, McColl BW, Pierozynski A, Monestier M, Pinteaux E, Rothwell NJ, Allan SM (2012) Neutrophil cerebrovascular transmigration triggers rapid neurotoxicity through release of proteases associated with decondensed DNA. J Immunol 189:381-392.

2. Amulic B, Hayes G (2011) Neutrophil extracellular traps. Curr Biol 21:R297-R298.

3. Arbel-Ornath M, Hudry E, Eikermann-Haerter K, Hou S, Gregory JL, Zhao L, Betensky RA, Frosch MP, Greenberg SM, Bacskai BJ (2013) Interstitial fluid drainage is impaired in ischemic stroke and Alzheimer's disease mouse models. Acta Neuropathol 126:353-364.

4. Barone FC, Hillegass LM, Price WJ, White RF, Lee EV, Feuerstein GZ, Sarau HM, Clark RK, Griswold DE (1991) Polymorphonuclear leukocyte infiltration into cerebral focal ischemic tissue: myeloperoxidase activity assay and histologic verification. J Neurosci Res 29:336-345.

5. Carare RO, Bernardes-Silva M, Newman TA, Page AM, Nicoll JA, Perry VH, Weller RO (2008) Solutes, but not cells, drain from the brain parenchyma along basement membranes of capillaries and arteries: significance for cerebral amyloid angiopathy and neuroimmunology. Neuropathol Appl Neurobiol 34:131-144

6. Chamorro A, Meisel A, Planas AM, Urra X, van de Beek D, Veltkamp R (2012) The immunology of acute stroke. Nat Rev Neurol 8:401-410.

7. Chen GY, Nuñez G (2010) Sterile inflammation: sensing and reacting to damage. Nat Rev Immunol 10:826-837.

8. Chu HX, Kim HA, Lee S, Moore JP, Chan CT, Vinh A, Gelderblom M, Arumugam TV, Broughton BR, Drummond GR, Sobey CG (2014) Immune cell infiltration in malignant

middle cerebral artery infarction: comparison with transient cerebral ischemia. J Cereb Blood Flow Metab 34:450-459.

9. Clark WM, Madden KP, Rothlein R, Zivin JA (1991) Reduction of central nervous system ischemic injury by monoclonal antibody to intercellular adhesion molecule. J Neurosurg 75:623-627.

10. Connolly ES Jr, Winfree CJ, Springer TA, Naka Y, Liao H, Yan SD, Stern DM, Solomon RA, Gutierrez-Ramos JC, Pinsky DJ (1996) Cerebral protection in homozygous null ICAM-1 mice after middle cerebral artery occlusion. Role of neutrophil adhesion in the pathogenesis of stroke. J Clin Invest 97:209-216.

11. Cserr HF, Harling-Berg CJ, Knopf PM (1992) Drainage of brain extracellular fluid into blood and deep cervical lymph and its immunological significance. Brain Pathol 2:269-276.

12. Cuartero MI, Ballesteros I, Moraga A, Nombela F, Vivancos J, Hamilton JA, Corbí AL, Lizasoain I, Moro MA (2013) N2 Neutrophils, novel players in brain inflammation after stroke: Modulation by the PPARγ agonist rosiglitazone. Stroke 44:3498-3508.

13. de la Rosa X, Cervera A, Kristoffersen AK, Valdés CP, Varma HM, Justicia C, Durduran T, Chamorro Á, Planas AM (2014) Mannose-binding lectin promotes local microvascular thrombosis after transient brain ischemia in mice. Stroke 45:1453-1459.

14. del Zoppo GJ, Mabuchi T (2003) Cerebral microvessel responses to focal ischemia. J Cereb Blood Flow Metab 23:879-894.

15. del Zoppo GJ, Schmid-Schönbein GW, Mori E, Copeland BR, Chang CM (1991) Polymorphonuclear leukocytes occlude capillaries following middle cerebral artery occlusion and reperfusion in baboons. Stroke 22:1276-1283.

16. Dirks M, Niessen LW, Huijsman R, van Wijngaarden J, Minkman MM, Franke CL, van Oostenbrugge RJ, Koudstaal PJ, Dippel DW. PRomoting ACute Thrombolysis in Ischemic StrokE (PRACTISE) Investigators (2007) Promoting thrombolysis in acute ischaemic stroke. Int J Stroke 2:151-159.

17. Engelhardt B, Ransohoff RM (2005) The ins and outs of T-lymphocyte trafficking to the CNS: anatomical sites and molecular mechanisms. Trends Immunol 26:485-495.

18. Enzmann G, Mysiorek C, Gorina R, Cheng YJ, Ghavampour S, Hannocks MJ, Prinz V, Dirnagl U, Endres M, Prinz M, Beschorner R, Harter PN, Mittelbronn M, Engelhardt B, Sorokin L (2013) The neurovascular unit as a selective barrier to polymorphonuclear granulocyte (PMN) infiltration into the brain after ischemic injury. Acta Neuropathol 125:395-412.

19. Fridlender ZG, Albelda SM (2012) Tumor-associated neutrophils: friend or foe? Carcinogenesis 33:949-955.

20. Fuchs TA, Brill A, Duerschmied D, Schatzberg D, Monestier M, Myers DD Jr, Wrobleski SK, Wakefield TW, Hartwig JH, Wagner DD (2010) Extracellular DNA traps promote thrombosis. Proc Natl Acad Sci U S A 107:15880-15885.

21. Garcia JH, Liu KF, Bree MP (1996) Effects of CD11b/18 monoclonal antibody on rats with permanent middle cerebral artery occlusion. Am J Pathol 148:241–248.

22. Garcia JH, Liu KF, Yoshida Y, Lian J, Chen S, del Zoppo GJ (1994) Influx of leukocytes and platelets in an evolving brain infarct (Wistar rat). Am J Pathol 144:188-199.

23. Gelderblom M, Leypoldt F, Steinbach K, Behrens D, Choe CU, Siler DA, Arumugam TV, Orthey E, Gerloff C, Tolosa E, Magnus T (2009) Temporal and spatial dynamics of cerebral immune cell accumulation in stroke. Stroke 40:1849-1857.

24. Hallenbeck JM, Dutka AJ, Tanishima T, Kochanek PM, Kumaroo KK, Thompson CB, Obrenovitch TP, Contreras TJ (1986) Polymorphonuclear leukocyte accumulation in brain regions with low blood flow during the early postischemic period. Stroke 17:246-253.

25. Hawkes CA, Härtig W, Kacza J, Schliebs R, Weller RO, Nicoll JA, Carare RO (2011) Perivascular drainage of solutes is impaired in the ageing mouse brain and in the presence of cerebral amyloid angiopathy. Acta Neuropathol 121:431-443.

26. Hawkes CA, Jayakody N, Johnson DA, Bechmann I, Carare RO (2014) Failure of perivascular drainage of β-amyloid in cerebral amyloid angiopathy. Brain Pathol 2:396–403.

27. Hernandez LA, Grisham MB, Twohig B, Arfors KE, Harlan JM, Granger DN (1987) Role of neutrophils in ischemia-reperfusion-induced microvascular injury. Am J Physiol 253:H699-703.

28. Hutchings M, Weller RO (1986) Anatomical relationships of the pia mater to cerebral blood vessels in man. J Neurosurg 65:316-325.

29. Howells DW, Porritt MJ, Rewell SS, O'Collins V, Sena ES, van der Worp HB, Traystman RJ, Macleod MR (2010) Different strokes for different folks: the rich diversity of animal models of focal cerebral ischaemia. J Cereb Blood Flow Metab 30:1412–3110.

30. Iadecola C, Anrather J (2011) The immunology of stroke: from mechanisms to translation. Nat Med 17:796-808.

31. Jaillon S, Galdiero MR, Del Prete D, Cassatella MA, Garlanda C, Mantovani A (2013) Neutrophils in innate and adaptive immunity. Semin Immunopathol 35:377-394.

32. Jiang N, Chopp M, Chahwala S (1998) Neutrophil inhibitory factor treatment of focal cerebral ischemia in the rat. Brain Res 788:25-34.

33. Kataoka H, Kim SW, Plesnila N (2004) Leukocyte-endothelium interactions during permanent focal cerebral ischemia in mice. J Cereb Blood Flow Metab. 24:668-676.

34. Krams M, Lees KR, Hacke W, Grieve AP, Orgogozo JM, Ford GA; ASTIN Study Investigators (2003) Acute Stroke Therapy by Inhibition of Neutrophils (ASTIN): an adaptive dose-response study of UK-279,276 in acute ischemic stroke. Stroke 34:2543-2548.

35. Malipiero U, Koedel U, Pfister HW, Levéen P, Bürki K, Reith W, Fontana A (2006) TGFbeta receptor II gene deletion in leucocytes prevents cerebral vasculitis in bacterial meningitis. Brain 129:2404-2415.

36. Mantovani A, Cassatella MA, Costantini C, Jaillon S (2011) Neutrophils in the activation and regulation of innate and adaptive immunity. Nat Rev Immunol 11:519-531.

37. Marín-Padilla M, Knopman DS (2011) Developmental aspects of the intracerebral microvasculature and perivascular spaces: insights into brain response to late-life diseases. J Neuropathol Exp Neurol 70:1060-1069.

38. Massberg S, Grahl L, von Bruehl ML, Manukyan D, Pfeiler S, Goosmann C, Brinkmann V, Lorenz M, Bidzhekov K, Khandagale AB, Konrad I, Kennerknecht E, Reges K, Holdenrieder S, Braun S, Reinhardt C, Spannagl M, Preissner KT, Engelmann B (2010) Reciprocal coupling of coagulation and innate immunity via neutrophil serine proteases. Nat Med 16:887-896.

39. Meves SH, Muhs A, Federlein J, Buttner T, Przuntek H, Postert T (2002) Recanalization of acute symptomatic occlusions of the internal carotid artery. J Neurol 249:188–192.

40. Müller I, Munder M, Kropf P, Hänsch GM (2009) Polymorphonuclear neutrophils and T lymphocytes: strange bedfellows or brothers in arms? Trends Immunol 30:522-530.

41. Nathan, C (2006) Neutrophils and immunity: challenges and opportunities. Nature Rev Immunol 6:173–182.

42. Papayannopoulos V, Zychlinsky A (2009) NETs: a new strategy for using old weapons. Trends Immunol 30:513-521.

43. Pérez-de Puig I, Miró F, Salas-Perdomo A, Bonfill-Teixidor E, Ferrer-Ferrer M, Márquez-Kisinousky L, Planas AM (2013) IL-10 deficiency exacerbates the brain inflammatory response to permanent ischemia without preventing resolution of the lesion. J Cereb Blood Flow Metab 33:1955-1966.

44. Pollock H, Hutchings M, Weller RO, Zhang ET (1997) Perivascular spaces in the basal ganglia of the human brain: their relationship to lacunes. J Anat 191:337-346.

45. Prestigiacomo CJ, Kim SC, Connolly ES Jr, Liao H, Yan SF, Pinsky DJ (1999) CD18-mediated neutrophil recruitment contributes to the pathogenesis of reperfused but not nonreperfused stroke. Stroke 30:1110-1117.

46. Rha JH, Saver JL (2007) The impact of recanalization on ischemic stroke outcome: a meta-analysis. Stroke 38:967-973.

47. Rørvig S, Honore C, Larsson LI, Ohlsson S, Pedersen CC, Jacobsen LC, Cowland JB, Garred P, Borregaard N (2009) Ficolin-1 is present in a highly mobilizable subset of human neutrophil granules and associates with the cell surface after stimulation with fMLP. J Leukoc Biol 86:1439-1449.

48. Stowe AM, Adair-Kirk TL, Gonzales ER, Perez RS, Shah AR, Park TS, Gidday JM (2009) Neutrophil elastase and neurovascular injury following focal stroke and reperfusion. Neurobiol Dis 35:82-90.

49. Wang Y, Li M, Stadler S, Correll S, Li P, Wang D, Hayama R, Leonelli L, Han H, Grigoryev SA, Allis CD, Coonrod SA (2009) Histone hypercitrullination mediates chromatin decondensation and neutrophil extracellular trap formation. J Cell Biol 184:205-213.

50. Weller RO, Kida S, Zhang ET (1992) Pathways of fluid drainage from the brain--morphological aspects and immunological significance in rat and man. Brain Pathol 2:277-284.

51. Zanette EM, Roberti C, Mancini G, Pozzilli C, Bragoni M, Toni D (1995) Spontaneous middle cerebral artery reperfusion in ischemic stroke: a follow-up study with transcranial Doppler. Stroke 26:430–433.

52. Zhang RL, Chopp M, Chen H, Garcia JH (1994) Temporal profile of ischemic tissue damage, neutrophil response, and vascular plugging following permanent and transient (2H) middle cerebral artery occlusion in the rat. J Neurol Sci 125:3-10.

53. Zhang RL, Chopp M, Jiang N, Tang WX, Prostak J, Manning AM, Anderson DC (1995) Anti-intercellular adhesion molecule-1 antibody reduces ischemic cell damage after transient but not permanent middle cerebral artery occlusion in the Wistar rat. Stroke 26:1438-1442.

54. Zhang ET, Inman CB, Weller RO (1990) Interrelationships of the pia mater and the perivascular (Virchow-Robin) spaces in the human cerebrum. J Anat 170:111-123.

Figure legends

Fig. 1. Identification of neutrophils in the brain after ischemia by flow cytometry. a,b) Flow cytometry gates of brain cells for representative mice after cauterization (c-MCAo) (a) and intraluminal (il-MCAo) occlusion (b), at the indicated time points and in a control non-ischemic brain (top of panel a). Cell populations are first identified by side and forward scatter (SSC and FSC) (left graphs), followed by the expression of CD11b and CD45, which shows a progressive increase of myeloid cells ($CD11b^{hi}CD45^{hi}$) (middle graphs) in the ischemic brain tissue. Separation of the latter population by CD11b and Ly6G allows the identification of neutrophils ($CD11b^{hi}$Ly6G+) (graphs on the right of each panel). The percentage of cells in each gate is indicated in the graphs. a) After illustrating the gating strategy from left to right, the panel on the right shows from top to bottom the increase in neutrophils (gate $CD11b^{hi}$ Ly6G+) with time after c-MCAo. b) Neutrophils are also found in the il-MCAo model (right panel). c) Quantification of brain tissue neutrophil numbers obtained after 10 min (n=2), 3 (n=5) and 15 (n=9) hours, and 1 (n=8), 2 (n=3), and 15 (n=2) days after c-MCAo are shown for the ipsilateral and contralateral hemispheres. Two-way ANOVA by time and hemisphere followed by the Bonferroni post-hoc test shows significant increases at 1 day in the ispilateral versus the contralateral hemisphere (*** $p<0.001$). The increase in neutrophil number seen 24h after c-MCAo (n=8) in the ipsilateral hemisphere was not detected after sham operation (n=5) (Mann-Whitney test, ** $p<0.005$). d) Quantification of brain tissue neutrophil numbers obtained in the ipsilateral and contralateral hemispheres 1 day after il-MCAo (n=8) or sham-operation (sham) (n=2). Two-way ANOVA by surgery (MCAo vs sham) and hemisphere followed by Bonferroni post-hoc test shows a significant increase of neutrophils in the ipsilateral hemisphere after il-MCAo (*$p<0.05$).

Fig. 2. Neutrophils in the brain after cauterization of the MCA (c-MCAo). a) Polymorphonuclear cells (PMNs) on the brain surface and reaching the Virchow-Robin space of an occluded cortical arteriole containing erythrocytes (white) in the vessel lumen. All the cell nuclei are stained with DAPI and the characteristic multilobular nucleus of PMNs is apparent surrounding the cortical arteriole. (b-m) NIMP-R14+ cells (green) and (n-u) Ly6G+ cells (green). b-f) NIMP-R14+ leukocytes cross the glia limitans (GFAP, red; pan-laminin, blue) in the ipsilateral hemisphere at 6h (b) and 15h (c,d), but they are not seen in the contralateral hemisphere (e,f). g) NIMP-R14+ cells located underneath the parenchymal basal lamina (red, pan-laminin) along the vessel wall in cortical layer I after 6h of ischemia. Images z_1-z_3 are confocal 1 μm-thick sections along the z axis. h-j) NIMP-R14+ cells (arrowheads) are seen on the parenchymal basal lamina of the ischemic cortex and along the vessels in the superficial cortical layers (h). A detail of the cells on the parenchymal cortical basal lamina is shown in (i) and the cellular invasion to the perivascular space of the cortical arterioles located in the core of infarction is illustrated in (j). Red is pan-laminin; blue shows all the cell nuclei with To-Pro3. k) NIMP-R14+ cells lie on the endothelial basal lamina (EBL, blue, α4-laminin) that surrounds the endothelium (E, red, Glut-1). l-m) NIMP-R14+ cells accumulate in perivascular spaces (arrows) and extravasate to the parenchyma of the infarcted core (arrowheads) while erythrocytes (white in l) remain in the vessel lumen. Red is pan-laminin. n-o) Ly6G+ neutrophils surrounding and outside a large leptomeningeal vessel (n), and extravasated from a leptomeningeal vessel (o). Erythrocytes (purple) are contained inside the vessel lumen. Blue is PDGFRβ. p,s) Neutrophils in the infarcted core located in the perivascular space between the endothelial (red, α4-laminin, EBL) and the parenchymal (blue, pan-laminin, PBL) basal laminae of blood vessels containing erythrocytes (purple) 24h after MCAO. q-r) Neutrophils surround the basal lamina of blood vessels (red, pan-laminin) in perivascular spaces and are free in the parenchyma of the infarcted core (arrowheads). t-u) Neutrophils in perivascular spaces of a cortical vessel (t) and a

leptomeningeal arteriole (u), and free (arrowheads) in the infarcted parenchyma. Red is α4-laminin and blue is To-Pro3. The time after c-MCAo is indicated in each panel. Number of mice at 6h, 15h and 24h are 3, 3, and 6, respectively. Bar scale: a-g, i, k, m, p-u: 10 μm; j, o: 20 μm; h, n: 50 μm.

Fig. 3. Neutrophils in the brain after permanent intraluminal MCAo (il-MCAo). (a-g) NIMP-R14+ cells (green) and (h-q) Ly6G+ cells (green). (a-b) NIMP-R14+ cells (arrowheads) are seen in the leptomeninges outside a vein (blue, α4-laminin) and an arteriole (red, Glut-1) at the ventral part of the brain and in the infarcted brain parenchyma. (c) A similar phenomenon is observed in this region after staining the glia limitans (red, GFAP; blue, pan-laminin). (d-g) NIMP-R14+ cells (blue are the nuclei; To-Pro3) are seen adjacent to the basal lamina (red, pan-laminin) of an arteriole in the dorsal cortex (d), nearby a small blood vessel (e), extravasated in the cortical parenchyma at the ventral part of the brain (f), and in the capillary lumen (g), where spread and punctuate staining is seen suggesting intravascular degranulation. (h-j) Ly6G+ neutrophils on the parenchymal basal lamina of the dorsal cortex (h), in perivascular spaces and lumen of a cortical arteriole (i), and in the ventral leptomeninges (j). Red (pan-laminin) shows the basal laminae, and blue shows the cell nuclei (To-Pro3). (k-n) Ly6G+ neutrophils are seen in the ventral leptomeninges (k), trapped in the lumen of a blood vessel in the ischemic striatum (l), and in perivascular spaces between the endothelial basal lamina (EBL, red, α4-laminin) and the parenchymal basal lamina at the margins of the infarcted cortical region (PBL, blue, pan-laminin) in the ventral part of the brain. o) Ly6G+ neutrophils at the cortical parenchymal basal lamina (red, pan-laminin) and in cortical layer I within the dorsal part of the brain at the margins of infarction. Cell nuclei are shown in blue (To-Pro3). p-q) Neutrophils (arrowheads) along blood vessels in the dorsal cortex (p) and extravasated in the parenchyma in the ventral part of the brain (q). Red is α4-laminin and blue is pan-laminin. The time after il-MCAO is indicated in each panel. Number

of mice at 6h and 24h are 5 and 8, respectively. Bar scale in a: 20 μm; b: 15 μm; c: 30 μm; d-q: 10 μm.

Fig. 4. Regional localization of neutrophils in the experimental MCAo models. The macroscopic appearance of the infarction is illustrated with MRI brain images (T2 maps) of mice 24 hours after c-MCAo (a) and il-MCAo (d) showing a pale area corresponding to the infarcted region. Squares in the MRI images indicate the approximate zones from where the microscopic images were obtained. Green is Ly6G; red is pan-laminin in all panels excepting in panel j, which is Glut-1; blue illustrates the nuclei stained with ToPro-3. For the c-MCAo model (n=6), a cortical zone at the margin of infarction is shown in (b). The dashed line is drawn to indicate the margins of infarction as assessed from the apparent difference in intensity of blood vessel basal lamina staining with pan-laminin. Ly6G+ neutrophils are abundant at the leptomeninges (arrow), and are only seen in the cortex (arrowhead) within the infarcted region. c) Cortical infarcted region showing abundant Ly6G+ neutrophils in the leptomeninges (arrow) and in the cortex (arrowhead). For the il-MCAo model (n=8), neutrophils are seen in the leptomeninges and mainly in marginal zones of the infarcted tissue as illustrated with images corresponding to the dorsal (e), lateral (f), and ventral (g,h) parts of the cortex, where neutrophils are seen associated to the parenchymal basal lamina or vessels (arrows), and are also seen free in the parenchyma (arrowheads). Neutrophils in the striatum (i) are mainly seen inside the vasculature (i1, i2) and only very rarely they are free in the infarcted striatal parenchyma (arrowhead in i3). Occasionally, neutrophils (arrowheads) are seen in the choroid plexus (arrow) (j1) and surrounding white matter (j2) in mice with very large infarctions. Bar scale: 30 μm (excepting in e1, e3, g1, i2, i3, and j2: 15 μm).

Fig. 5. Some neutrophils show histone-3 citrullination (Cit-H3) 24 hours after MCAo. (a-b, d-e) c-MCAo model (n=6) and (c, f) il-MCAo model (n=8). (a-c) Cit-H3+ neutrophils are seen

at perivascular locations (a) and extravascular (b) in the infarcted cortex, but they are located inside blood capillaries in the infarcted striatum (c). The shape of the vessels (blue) is apparent after staining PDGFRβ (a, b), which labels the surrounding pericytes, or pan-laminin (c) labeling the basal lamina. d) Illustrates a neutrophil (green, Ly6G+) (arrowhead) showing histone-3 citrullination (red, Cit-H3) extending outside the cell body together with DNA (blue, DAPI) (arrow). The phase contrast image merged with the fluorescence images and z-projections is shown on the right to illustrate co-localization of markers in the same cell. The neutrophil extracellular projections were occasionally directed towards isolated dense elements with a shape and size compatible with isolated erythrocytes (*) free in the parenchyma. e) Two neutrophils (green, Ly6G+) (arrowheads), one of them (left) shows a polymorphonuclear structure with DAPI staining (blue), while the other (right, arrow) shows a diffuse nuclear structure indicative of chromatin decondensation and is positive for Cit-H3 (red). f) A neutrophil (green, Ly6G+) (arrowhead) inside a capillary (blue, α4-laminin) is positive for Cit-H3 (red) and shows most of the DNA (white, DAPI) and Cit-H3 outside the cell (arrow) forming structures suggestive of intravascular NETosis. Bar scale: a-b: 20 μm; c: 10 μm; d-f: 5 μm.

Fig. 6. Polymorphonuclear cells in human stroke. Representative hematoxylin & eosin paraffin sections of the 3 stroke patients: (a-d) patient 1; (e,f) patient 2; (g,h) patient 3. a) Leptomeninges nearby the infarcted region. Dark purple cells morphologically compatible with polymorphonuclear cells (PMNs) are abundant in the leptomeninges adjacent to the infarction. b) PMNs are not apparent in the leptomeninges adjacent to non-affected tissue and distant from the infarction. c,d) PMNs are seen in the vessels (arrows) and in marginal zones of the infarcted parenchyma (arrowhead) in the temporal lobe. e) PMNs are seen in the leptomeninges proximal to the infarcted core in the cerebellum. f) PMNs are seen associated to blood vessels (arrow) and extravasated from the vasculature (arrowhead). g)

PMNs located inside and surrounding a large meningeal vessel in the cerebellum. The inset is magnified in panel h showing the adjacent infarcted cerebellar parenchyma where an extravasated PMN is seen in the molecular cell layer. The asterisk indicates a red hypoxic Purkinje cell. Insets illustrate the cells in more detail after magnification of the area inside the box in each picture (x2 in d; x2.5 in a; x3 in e). Bar scale: (a, b, d-g) 20 μm; (c, h) 10 μm.

Fig. 7. Neutrophil elastase positive cells in human stroke. (a-d) Staining is shown for neutrophil elastase (green), laminin (red), DAPI (blue), and the merged images. a) Unaffected non-ischemic brain region showing an intravascular elastase+ cell (arrow). b) Infarcted core region showing perivascular elastase+ cell (arrow). c) Elastase+ cells extravasated at the meninges proximal to the ischemic tissue (arrow). d) Elastase+ cells extravasated from a vessel (arrow). e) Double staining with neutrophil elastase and myeloperoxidase (MPO) show colocalization in the same cell. Panel a is from patient number 2; b is from patient number 3; c-e are from patient number 4. f-h) Quantification of the number of neutrophil elastase+ cells per area in brain sections according to their intravascular, perivascular, or extravascular localization shows the values corresponding to a control non-affected region, the periphery of infarction, and the core of infarction, as well as the zone of the leptomeninges proximal to the core (ischemic) or to a non-affected region (control). Values are expressed as the mean ± SEM for n=3 patients. There was a non-significant trend to higher neutrophil elastase+ cell numbers/area in the core region versus the corresponding control region. A significant increase in neutrophil elastase+ cell numbers/area was found in the meninges adjacent to the ischemic tissue versus the meninges adjacent to the non-affected brain tissue. *$p<0.05$. Bar scale: 10 μm.

figure 1
Click here to download high resolution image

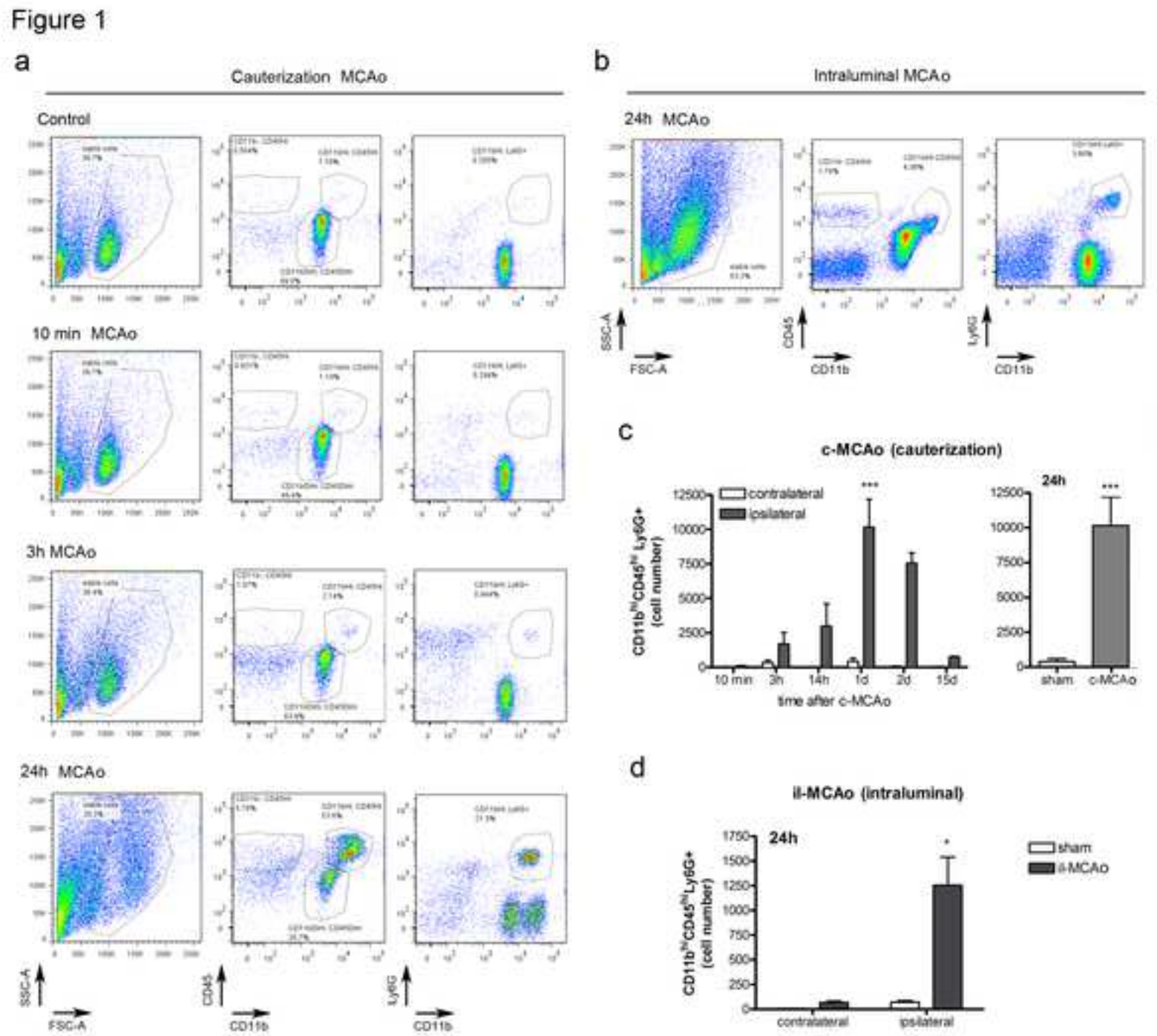

figure 2
Click here to download high resolution image

Figure 2

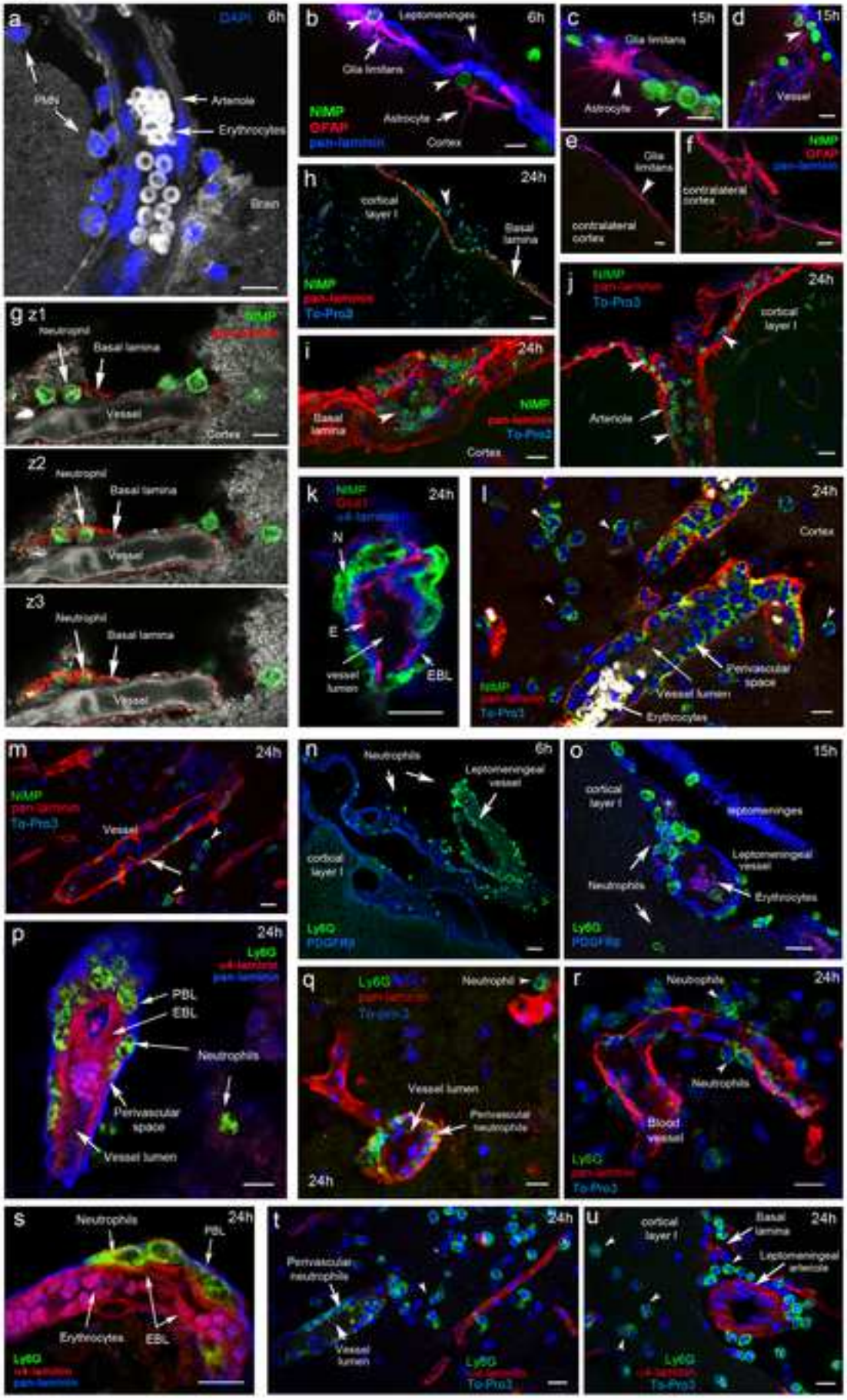

figure 3
Click here to download high resolution image

Figure 3

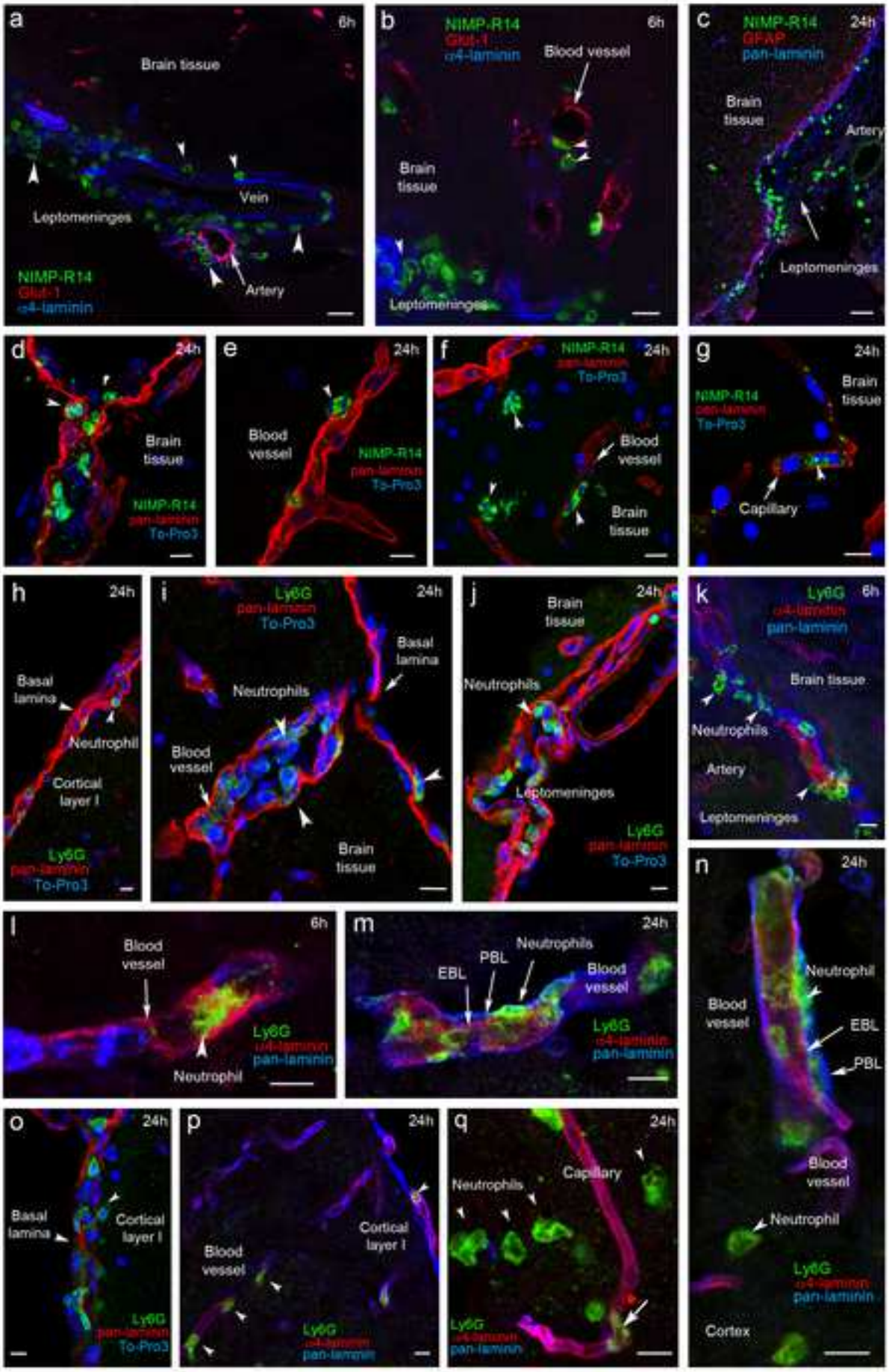

figure 4
Click here to download high resolution image

Figure 4

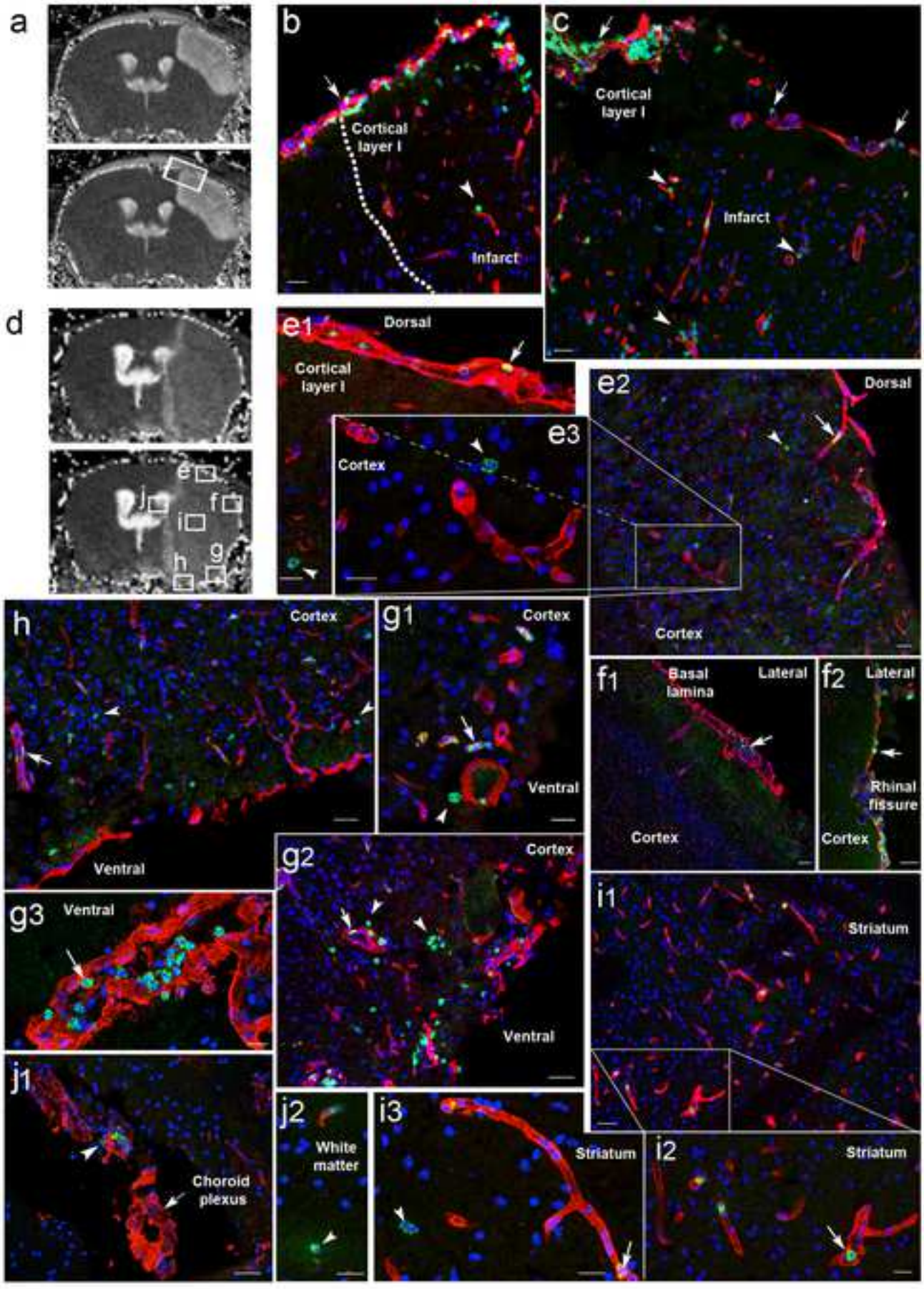

figure 5
Click here to download high resolution image

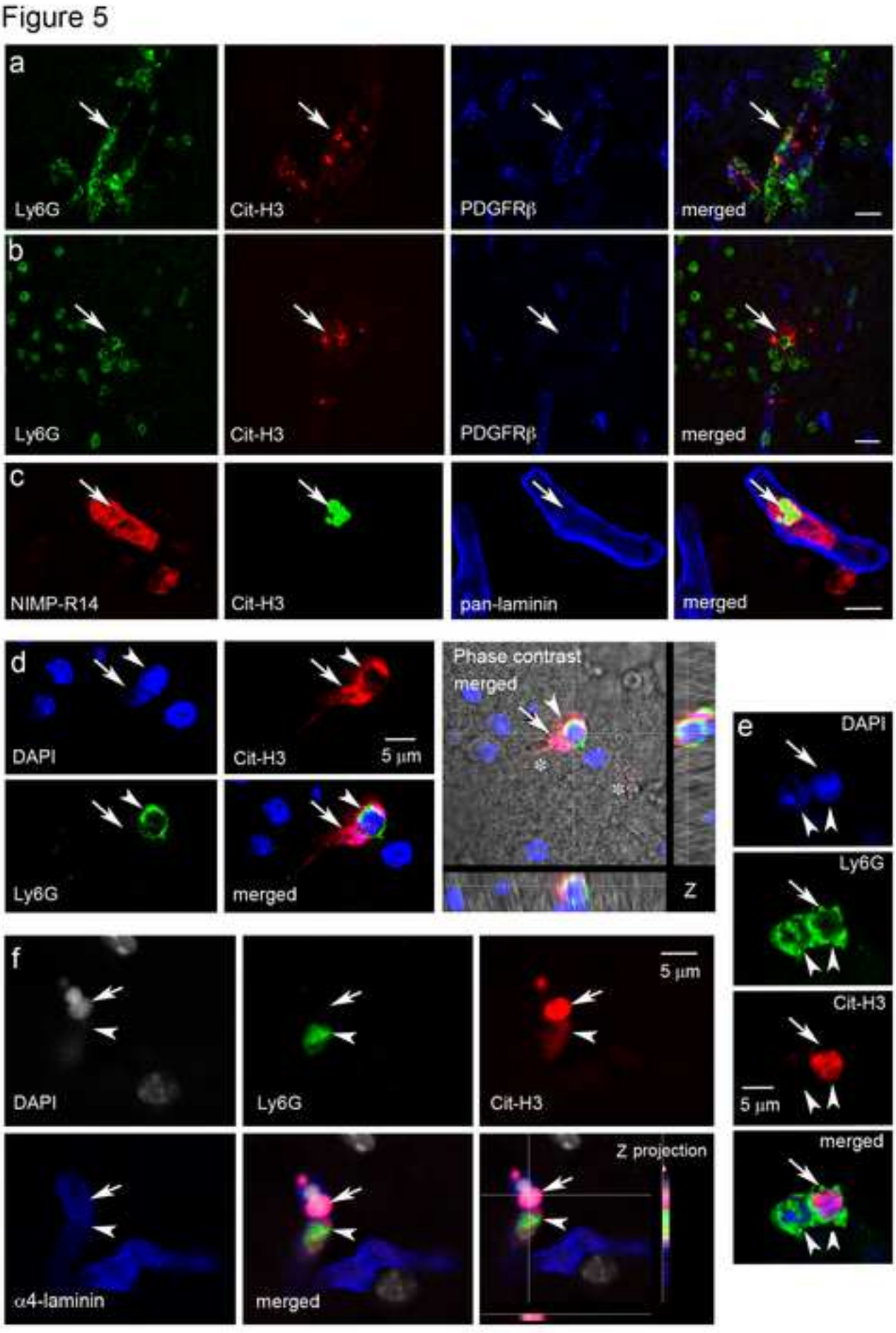

figure 6
Click here to download high resolution image

Figure 6

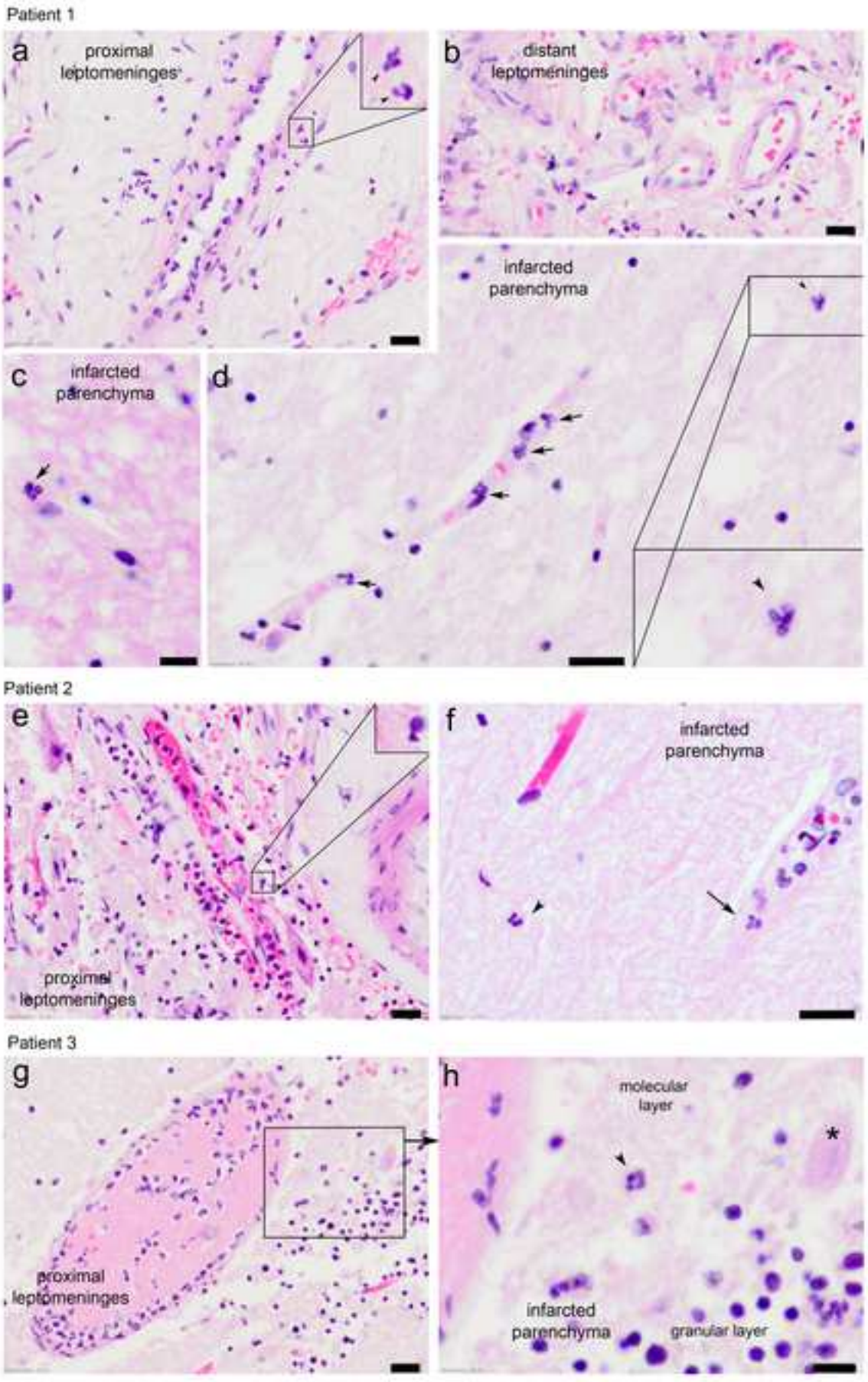

figure 7
Click here to download high resolution image

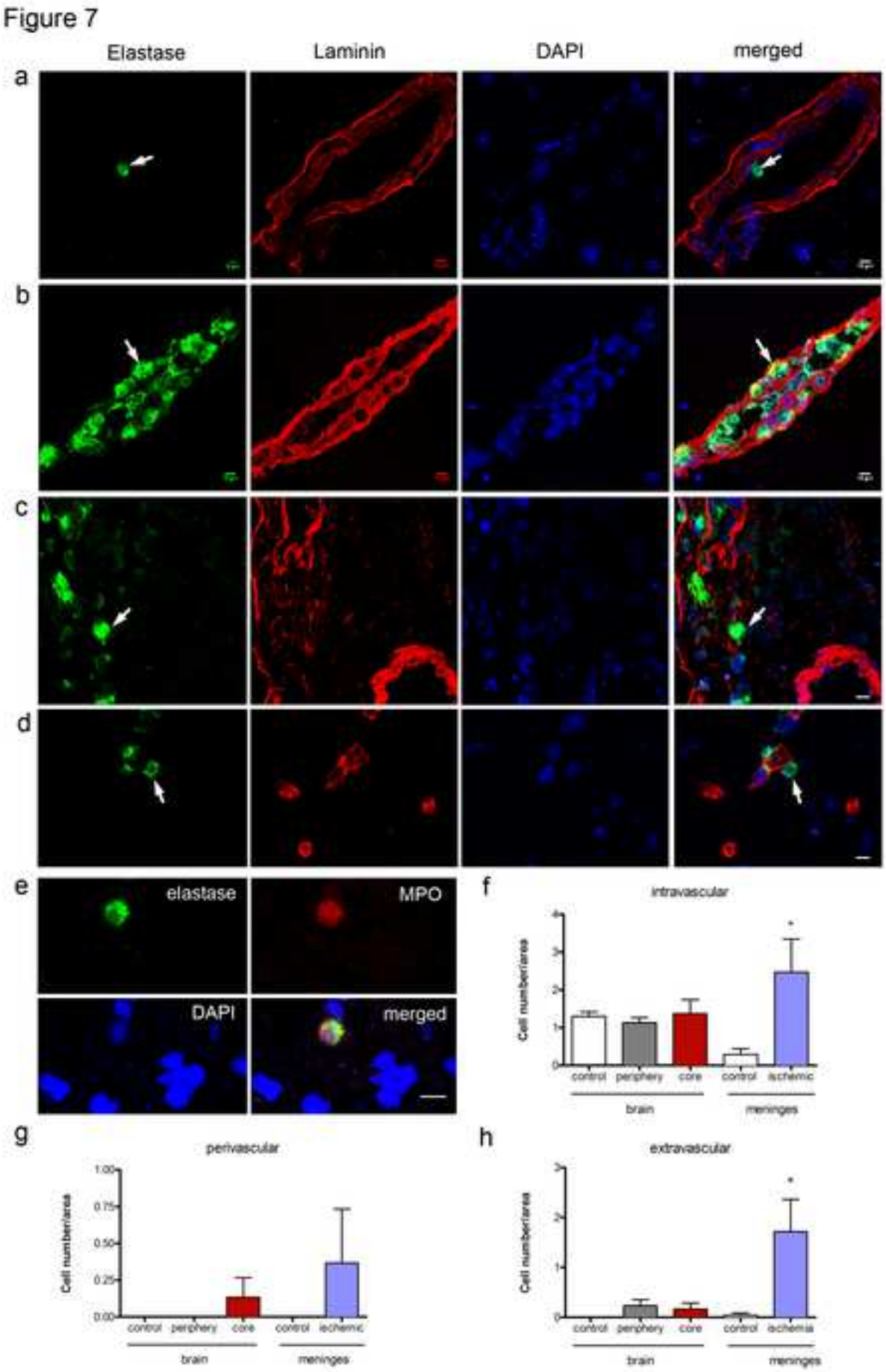

electronic supplementary material

Click here to download electronic supplementary material: Supplementary Material-rev2.pdf

ONLINE SUPPLEMENT

Neutrophil recruitment to the brain in mouse and human ischemic stroke

Isabel Perez-de-Puig[1&], Francesc Miró-Mur[2&], Maura Ferrer-Ferrer[1,2], Ellen Gelpi[3], Jordi Pedragosa[1], Carles Justicia[1,2], Xabier Urra[2,4], Angel Chamorro[2,4], Anna M. Planas[1,2]*

1 Department d'Isquèmia Cerebral i Neurodegeneració, Institut d'Investigacions Biomèdiques de Barcelona (IIBB), Consejo Superior de Investigaciones Científicas (CSIC), Barcelona, Spain.

2 Institut d'Investigacions Biomèdiques August Pi i Sunyer (IDIBAPS), Barcelona, Spain

3 Neurological Tissue Bank of the Biobanc-Hospital Clinic- IDIBAPS, Barcelona, Spain.

4 Functional Unit of Cerebrovascular Diseases, Hospital Clínic, Barcelona, Spain

& These authors equally contributed to this work

1) Supplementary Methods

Experimental brain ischemia

Focal brain ischemia was induced by permanent occlusion of the right middle cerebral artery (MCA) in mice, using two different techniques: either by cauterization of the distal portion of the MCA (c-MCAo) (n=43), or by filament intraluminal MCA occlusion (il-MCAo) (n=28). Anesthesia was induced with 4 % isoflurane in a mixture of 30% O_2 and 70% N_2O and it was maintained with 1-1.5 % isoflurane in the same mixture by the aid of a facial mask. The cauterization technique was carried out as previously reported [43]. Briefly, after drilling a small hole in the cranium at the level of the distal portion of the MCA, the artery elevated with a hook, was occluded by cauterization and was cut to ensure permanent blood flow interruption. Flow obstruction was visually verified. Animals showing subdural hemorrhages or signs of incorrect surgery were immediately excluded from the study (n=2 mice). After surgery, animals were allowed to recover from the anesthesia and were studied at different time points ranging from 10 min to 15 days following c-MCAo. None of the mice died during the study. For sham-operation (n=7), all surgical procedures were carried out but the MCA was not cauterized and the mice were killed at 24 hours. To exclude any effects due to cauterization, in a small group of mice (n=3) we carried out ligature of the MCA (8/0 black-braided silk suture) instead of cauterization, and the mice were studied 24 hours later.

Permanent il-MCAo was induced as previously reported [13], with modifications. Anesthesia was induced with 4 % isoflurane in a mixture of 30 % O_2 and 70 % N_2O and maintained with 1–1.5 % isoflurane in the same a mixture with a facial mask. A longitudinal cut was made in the ventral middle line of the neck to expose the right carotid territory. Next, the submaxillary glands and the omohyoid and sternohyoid muscles were separated, exposing the carotid vessels. The thyroid artery and occipital arteries were thermocoagulated. The right common carotid artery was firmly tied with a 6/0 silk suture and a 7/0 nylon

monofilament blunted at the tip (Suturas Arago, Spain) was introduced through the internal carotid artery to the level where the MCA branches out. The drop of cerebral blood flow was assessed with laser Doppler flowmetry (Perimed, Sweden). After surgery, the mice were kept under a heating lamp for approximately 30 min until they recovered from the anesthetic and they were killed 6, 15 or 24 hours after the occlusion. Three mice died before 24 hours after il-MCAo. Sham-operated mice (n=4) were subjected to surgery but the filament was only briefly introduced into the external carotid artery and was immediately removed, and mice were killed after 24 hours. Control mice (n=4) were naïve mice not subjected to surgery or anesthesia.

MRI was carried out in some of the animals to assess the infarction at 24h. MRI was performed in a 7.0 T BioSpec 70/30 horizontal animal scanner (Bruker BioSpin, Ettlingen, Germany), equipped with a 12-cm inner diameter actively shielded gradient system (400 mT/m). The receiver coil was a phased array surface coil for mouse brain. Mice were placed in a supine position in a Plexiglas holder with a nose cone for anesthesia administration (isoflurane in a mixture of 30% O_2 and 70% N_2O), fixed with a tooth and ear bars, and adhesive tape and maintained under controlled temperature during the acquisition period. Tripilot scans were carried out for accurate positioning of the animal's head in the isocenter of the magnet. T2 relaxometry maps were acquired with a multi-slice multi-echo acquisition sequence with 16 effective echo times from 11 to 176 ms, TR=4764 ms, FOV=20x20x6 mm^3, matrix size 256x256x18 pixels and spatial resolution 0.078x0.078x0.5 mm^3/pixel. Data were processed using Paravision 5.0 software (Bruker).

Isolation of cells from tissues

Mice were anesthetized and transcardially perfused with 40 mL saline. The ischemic brain tissue (ipsilateral to the MCAo) and the corresponding mirror regions of the non-ischemic hemisphere (contralateral) were dissected out and analyzed separately. For the c-MCAo

model the cortex was dissected out, whereas for the il-MCAo model the dissected tissue included the cortex and the striatum. The tissue was incubated for 30 minutes at 37°C in 2 mL of RPMI 1640 medium (Life Technologies S.A., Alcobendas, Madrid, Spain) containing 100 U/mL collagenase IV and 50 U/mL DNAse I. Brain tissue was passed through a tissue grinder and cells were recovered after centrifugation at 400 x*g* for 10 min at RT and separated from myelin and debris in 70 % and 30 % isotonic Percoll gradient (GE Healthcare) prepared in Hank's Balanced Salt Solution (HBSS) without calcium or magnesium. Samples were centrifuged at 1,000 x *g* for 30 min without acceleration or brake. Cells were collected from the interface, washed once with HBSS, and processed for flow cytometry.

Flow cytometry

Isolated brain cells were washed with fluorescence-activated cell sorting (FACS) buffer (phosphate-buffered saline, 2 mM EDTA, 2% FBS), incubated at 4 ºC for 10 min with FcBlock (1/200; Clone 2.4G2; BD Pharmingen), and incubated with primary antibodies in FACS buffer for 30 min at 4ºC. The antibodies used were rat anti-mouse CD11b (clone M1/70, Alexa Fluor 647, BD Pharmingen), CD45 (clone 30-F11, FITC, BD Pharmingen), and Ly6G (clone 1A8, PE-Cy7, BD Pharmingen). Isotype controls were rat IgG2bκ (clone A95-1, Alexa Fluor 647 or FITC, BD Pharmingen), rat IgG2a (FITC, Hycult Biotech), and rat IgG2aκ (clone R35-95, PE-Cy7, BD Pharmingen). Data acquisition was carried out in a BD FacsCantoII cytometer (BD Biosciences) using the FacsDiva software (BD Biosciences). Cells were morphologically identified by linear forward scatter (FSC-A) and side scatter (SSC-A) parameters. Data analysis was carried out with FlowJo software (version 7.6.5, TreeStar Inc., Ashland, OR, USA). Again, cells were plotted on forward versus side scatter and single cells were gated on FSC-A versus FSC-H linearity. Flow-Count Fluorospheres (Beckman-Coulter) were used for absolute cell number quantification.

2) Supplementary Figures

Supplementary Figure 1. Imaging of the intracranial occlusion site of patients (arrows).

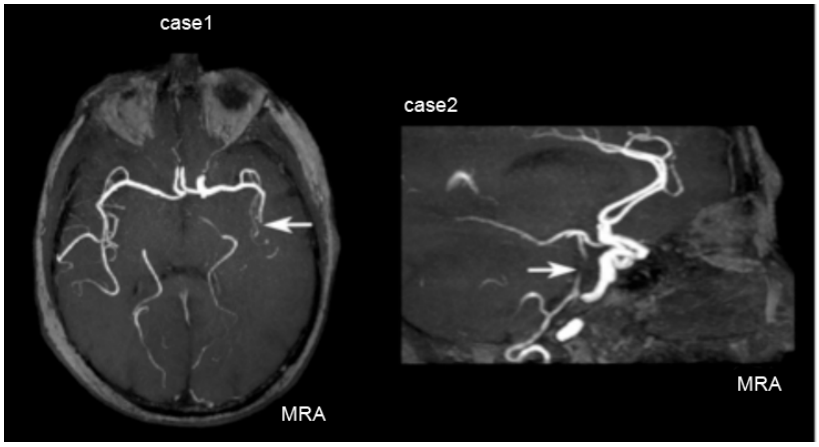

Images were obtained within the first day after stroke onset. Case 1 had a branch occlusion (M2) in the left middle cerebral artery. Case 2 had an occlusion of the middle segment of the basilar artery. MRA: magnetic resonance angiography.

Supplementary Figure 2. Schematic representation of the human brain regions that where dissected out.

The exact anatomic regional location varies from patient to patient depending on infarct localization. (1) Is the core of infarction, (2) is the periphery, and (3) is a non-ischemic region distant from the affected core.

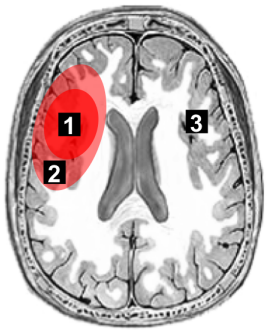

Supplementary Figure 3. Neutrophils in post-capillary venules and in the lumen of capillaries.

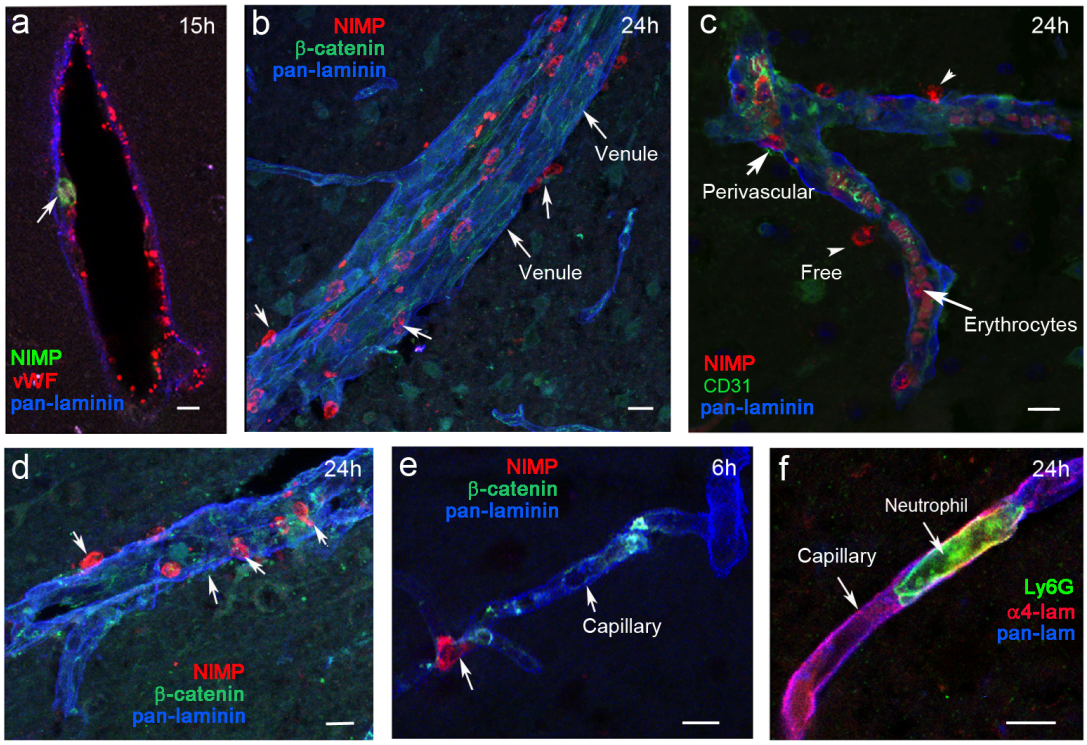

(a-e) Cauterization c-MCAo model and (f) intraluminal il-MCAo model. NIMP-R14+ or Ly6G+ cells, as indicated in each panel, are located in venules (a-d) or in the capillary lumen (e,f). Images are representative of n=9 mice for the c-MCAo model (n=3 at 15 hours and n=6 at 24 hours), and n=8 for the il-MCAo model. Bar scale: 10 μm.

Supplementary Figure 4. Ly6G+ cells express elastase**.**

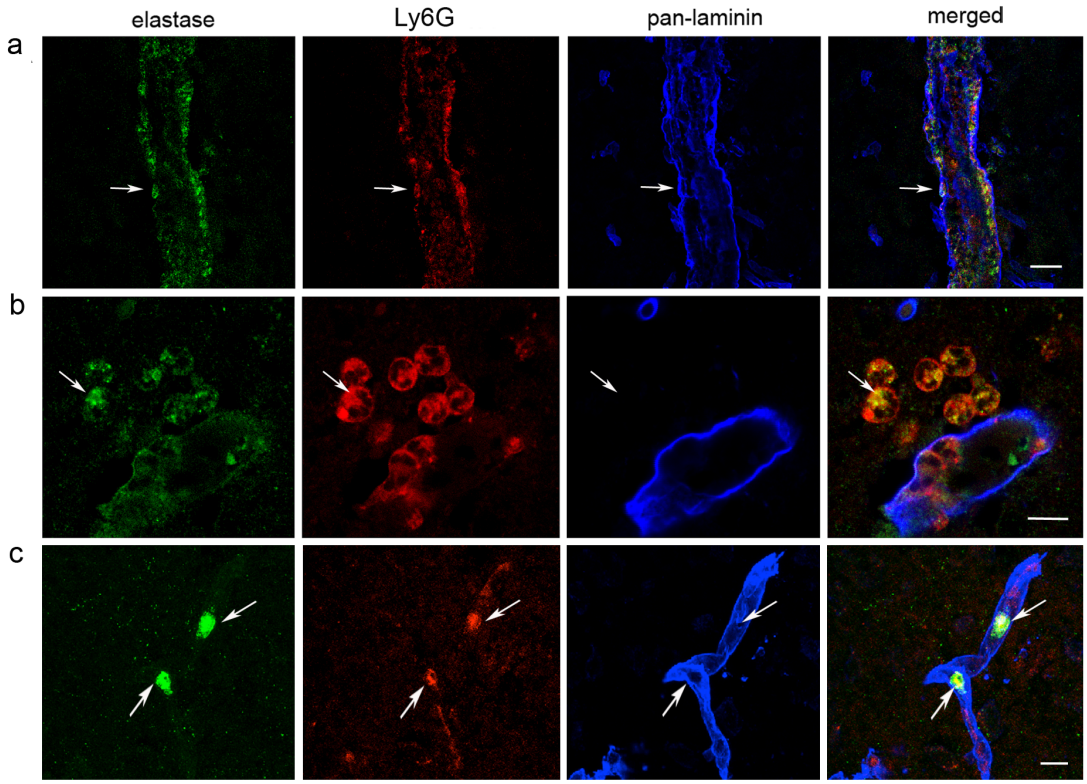

(a-b) Images are representative of mice for the cauterization c-MCAo model (n=6) and (c) intraluminal il-MCAo model (n=8). Ly6G+ cells are elastase+. Double stained cells are seen in perivascular spaces (a), extravasated in the parenchyma (b), and intravascularly (c). Bar scale: a, 25 μm; b-c, 10 μm.

Supplementary Figure 5. Signs of NET formation 24 hours after c-MCAo.

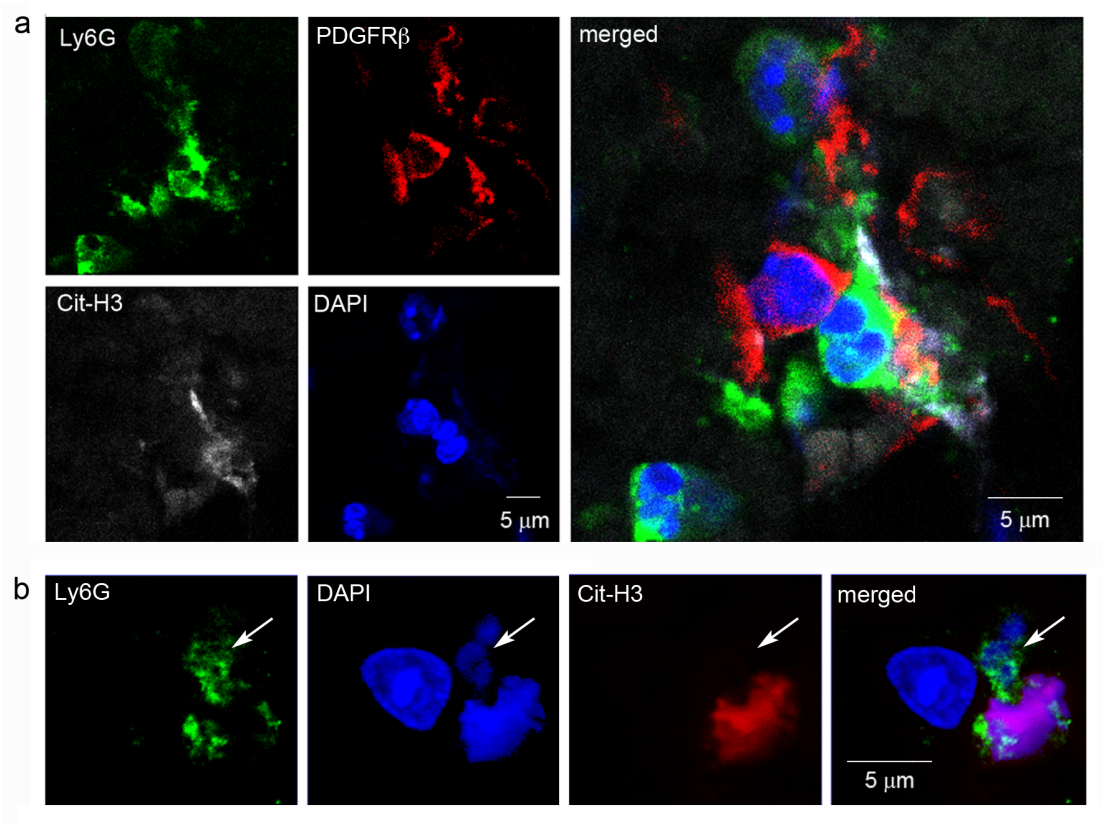

a) Perivascular neutrophils (green, Ly6G) nearby a pericyte (red, PDGFRβ) positive for Cit-H3 (white). DNA is shown in blue (DAPI). b) Neutrophil (green, Ly6G) showing Cit-H3 (red) in the nucleus (blue, DAPI) and expulsion of DNA (arrow). b) Images show two cells, one of them is Ly6G+ (green), shows a Cit-H3+ reaction, and expels cellular material (arrow) and DNA (blue, DAPI). Images are representative for n=6 mice 24h after c-MCAo. Bar scale: 5 μm.

Supplementary Fig. 6. Myeloperoxidase staining in human stroke tissue.

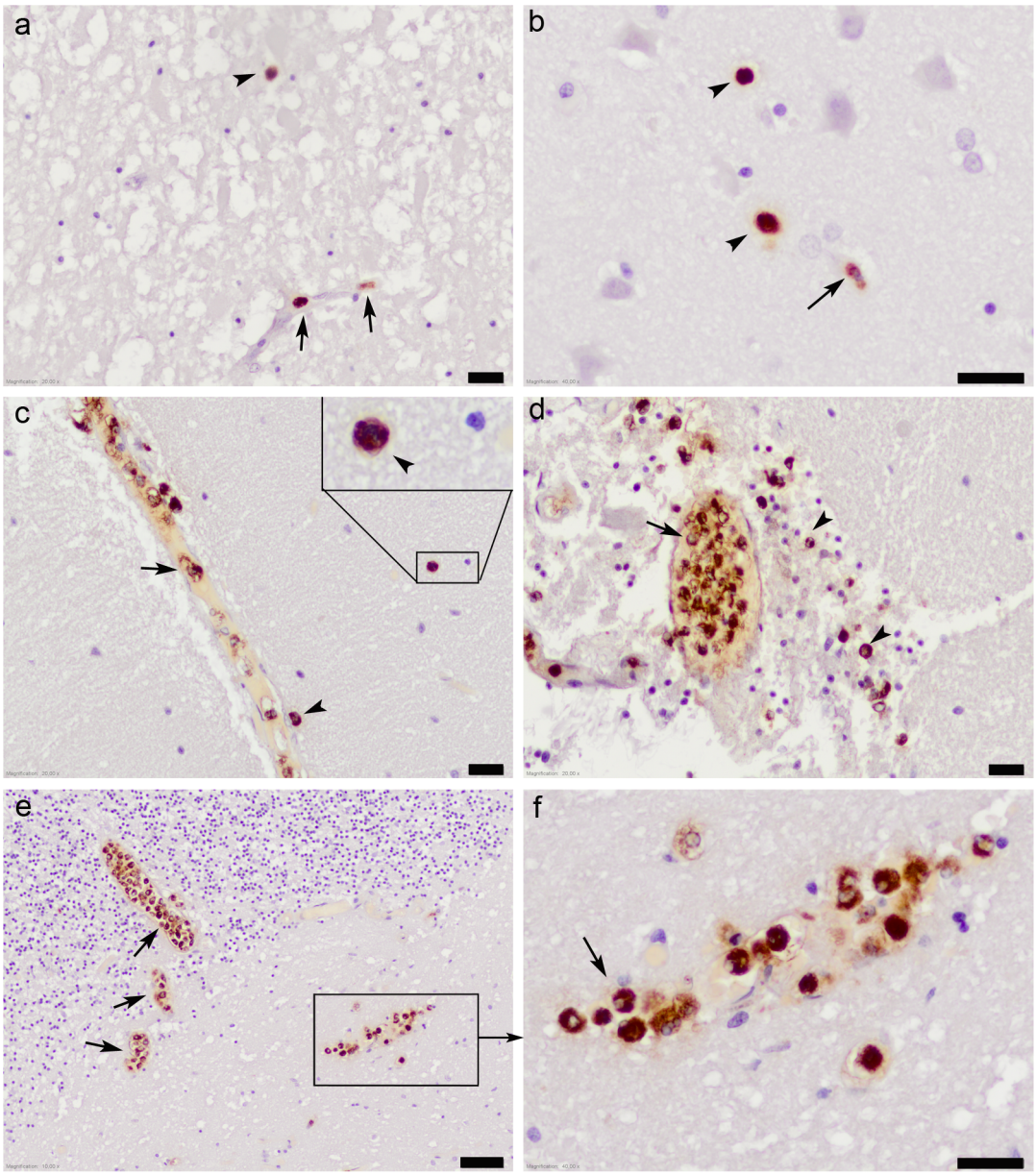

Myeloperoxidase (MPO) positive cells (dark brown) in paraffin sections of infarcted regions counterstained with hematoxylin (blue). Arrows indicate vascular or perivascular MPO+ cells and arrowheads point to MPO+ cells apparently free in the ischemic parenchyma. a, b) show the ischemic cortex in the temporal lobe region of patient number 1. c-f) show the ischemic cerebellum of patient number 2, illustrating MPO+ cells in a large vessel and in the parenchyma (c), in the leptomeninges proximal to infarction (d), and perivascularly in vessels of the infarcted cerebellar parenchyma (e, f). Inset in c corresponds to x3 magnification. Inset in e is shown at higher magnification in f illustrating a vessel in the infarcted cerebellar white matter. Bar scale: a-d, f: 20 μm; e: 50 μm.